Interfacial degradation of steel fibers in fiber-reinforced mortars under high-temperature exposure: A coupled thermo-mechanical-microstructural insight

Mohammmed Ezziane, Mohamed Sahraoui, Laurent Molez, Mostefa Hani, Ibrahim Messaoudene, Yazid Chetbani, Ahmed Belaadi, Ibrahim M.H. Alshaikh, Djamel Ghernaout

Results in Engineering 29 (2026) 108604

Contents lists available at ScienceDirect

Results in Engineering

journal homepage: www.sciencedirect.com/journal/results-in-engineering

Interfacial degradation of steel fibers in fiber-reinforced mortars under high-temperature exposure: A coupled thermo-mechanical-microstructural insight

Ezziane M. Mohammed [a], Mohamed Sahraoui [b], Molez L. Laurent [c], Mostefa Hani [d,e], Ibrahim Messaoudene [f], Yazid Chetbani [g], Ahmed Belaadi [h,*], Ibrahim M.H. Alshaikh [i,*], Djamel Ghernaout [j,k]

[a] Laboratoire matériaux (LABMAT), Ecole Nationale Polytechnique d'Oran Maurice Audin, 31000 Oran, Algérie
[b] Institute of Architecture and Urbanism, Saad Dahlab Blida 1 University, Algeria
[c] INSA – Université Européenne de Bretagne 20, avenue des Buttes de Coësmes, CS 70839, F35708 Rennes cedex, France
[d] Department of Civil Engineering, Eskisehir Technical University, 26555, Eskisehir, Türkiye
[e] Department of Civil Engineering and Hydraulics, Faculty of Sciences and Technology, Jijel University, P.O. Box 98, 18000 Jijel, Algeria
[f] Geomaterials Laboratory (LDGM), M'sila University, 28000, Algeria
[g] Centre de Recherche scientifique et Technique en Analyses Physico-Chimiques CRAPC, Technical platform for physicochemical analysis, University center N°02, University of Laghouat 03000, Algeria
[h] Department of Mechanical Engineering, Faculty of Technology, University 20 Août 1955-Skikda, El-Hadaiek Skikda, Algeria
[i] Department of Civil Engineering, University of Science and Technology, Faculty of Engineering, Sana'a, Yemen
[j] Chemical Engineering Department, College of Engineering, University of Ha'il, PO Box 2440, Ha'il 81441, Saudi Arabia
[k] Chemical Engineering Department, Faculty of Engineering, University of Blida, PO Box 270, Blida 09000, Algeria

ARTICLE INFO

Keywords:
Steel fibers
High temperature
Bond degradation
Flexural strength
Pullout test
Oxidation
SEM analysis
Fire resistance

ABSTRACT

This study examines the thermal degradation of steel fiber reinforced mortars (SFRM) within the temperature range of 20 to 800°C, with emphasis on the evolution of the interfacial bond between steel fibers and the cementitious matrix. A layered four point flexural pullout configuration was introduced to measure temperature dependent interfacial shear stress under controlled loading, offering greater precision than conventional pullout methods. The work identifies a critical transition near 500°C where bond capacity declines rapidly, a mechanism that has not been fully characterized in earlier research. Mechanical evaluation included flexural strength and residual modulus, while microstructural assessment employed Scanning Electron Microscopy (SEM), Energy Dispersive X-ray Spectroscopy (EDS), and Thermogravimetric Analysis (TGA). The results show that steel fibers improve initial flexural strength and crack bridging capacity, and that the interface remains stable up to about 400°C. Above this level, shear resistance decreases due to oxidation of the fiber surface and dehydration of the surrounding matrix. At 800°C, most of the fiber cross section converts into brittle oxides, leading to complete loss of anchorage and clear interfacial separation. SEM and EDS confirm oxide layer growth and matrix vitrification, and TGA reveals mass losses approaching 65 % under oxidizing conditions. The study also shows that phosphate coatings on steel fibers lose stability above 420°C, limiting their protective function. The combined mechanical and microstructural findings clarify the processes that govern bond deterioration in steel fiber reinforced mortars at high temperature and support the development of improved reinforcement strategies for fire exposed cementitious composites.

1. Introduction

Modern structures need materials that can withstand fire because extreme heat in tunnels, parking areas, and tall buildings can severely damage concrete [1,2]. Among the forms of thermal damage, explosive spalling is the most harmful because rapid heating causes surface layers to break away under trapped vapor pressure [3,4]. Earlier work by Kalifa et al. [5] and Hertz [6] showed that dense concretes with limited

* Corresponding authors.
E-mail addresses: a.belaadi@univ-skikda.dz (A. Belaadi), ibrahimalshaikh86@gmail.com (I.M.H. Alshaikh).

https://doi.org/10.1016/j.rineng.2025.108604
Received 28 August 2025; Received in revised form 19 November 2025; Accepted 4 December 2025
Available online 5 December 2025

porosity are more prone to damage because trapped vapor cannot escape, which raises internal stress and leads to tensile failure. At high temperature the oxidation of steel fibers and the weakening of their interface with the matrix become important factors that influence durability. Studies report that steel fiber reinforced concrete can still lose a large share of its compressive strength, reaching reductions close to 78.99 % at 900°C 78.99 % [7]. The use of waste steel fibers can slow strength loss, with some mixtures retaining more than 44 % of their initial capacity at very high temperatures [8]. Interfacial damage caused by chemical attack, hydrolysis, and surface breakdown weakens the bond between the fibers and the surrounding matrix [9], and this process is accelerated by the movement of hydroxyl and chloride ions [10]. Coatings such as pyrolytic carbon and silicon carbide have been developed to improve oxidation resistance and extend fiber durability in harsh conditions [11]. These treatments can repair minor defects, yet their performance still varies with environmental and thermal exposure, which limits their reliability in long term applications.

The bond between steel fibers and the cementitious matrix plays a central role in the residual performance of fiber reinforced systems [12]. This bond weakens under heating because oxidation, matrix microcracking, and chemical changes reduce adhesion at the interface [13–15]. Fang et al. [16] showed that bond slip behavior controls the contribution of fibers during loading, with hooked end fibers providing better anchorage than straight fibers, particularly at elevated temperature. Giaccio and Zerbino [17] reported that fiber reinforced concrete maintains higher flexural capacity than plain concrete after heating, and Colombo et al. [18] observed similar trends in thin structural elements. These studies confirm that steel fibers improve mechanical response, yet they also highlight that interfacial degradation becomes the main limitation as temperature rises. Once temperatures exceed roughly 500–600°C, oxidation of the fiber surface and thermal incompatibility with the matrix reduce load transfer, making bond failure a key factor governing post fire behavior [19–22].

Recent investigations have strengthened this understanding. Caravello et al. [23] and Tong et al. [24] showed through SEM and pullout testing that oxidation at high temperature produces clear microstructural damage within the interfacial transition zone. This damage reduces anchorage and causes a gradual loss of bond strength. Ahmad et al. [25] reported that steel fibers improve fracture resistance up to about 500°C, yet differences in thermal expansion between the fibers and the surrounding matrix promote microcracking and localized spalling as the temperature increases. These findings indicate that the main factor controlling the post fire response of steel fiber reinforced composites is interfacial degradation rather than deterioration of the bulk matrix.

Although many studies have highlighted the benefits of steel fibers, the processes that govern their interfacial degradation at high temperature are still not fully understood. Most earlier work has focused on compressive and flexural behavior, while changes in chemistry and microstructure at the interface have received less attention [16,19–22]. Above 400°C, matrix dehydration, cracking, and fiber oxidation weaken the interfacial transition zone and accelerate debonding. Coatings such as zinc phosphate improve corrosion resistance under normal conditions, yet their performance at elevated temperature remains uncertain. Pi et al. [26] reported that nano silica modified fibers improve tensile response at various water to cement ratios, and recent studies by Tchekwagep et al. [27] and Tong et al. [24] showed that treated or galvanized fibers delay oxidation and help maintain bond strength during heating. Pullout tests and SEM observations support these improvements, although issues related to coating uniformity, processing cost, and thermal compatibility still limit their use. The effectiveness of zinc phosphate treatments also depends on the processing temperature. Liu et al. [28] noted that coating stability decreases when treatment temperatures rise, which increases surface porosity and makes fibers more sensitive to oxidation. At higher temperature the loss of hook geometry, reduction in yield strength, and surface roughening further reduce anchorage. The combined effects of thermal mismatch and matrix dehydration promote microcracking and lead to earlier debonding. Despite ongoing research, the interactions between oxidation, microstructural changes, and bond loss in coated steel fibers require clearer understanding.

This study advances current understanding of fiber-to-matrix interaction under thermal loading, with specific emphasis on steel fiber-reinforced mortars. Related work has examined the influence of temperature, microstructural, and mechanical behaviors on other cementitious and composite systems such as granular soils, sprayed and self-compacting concretes, pykrete, compressed earth blocks, recycled aggregates, marble powder-based concrete, sustainable high-performance concrete, and sisal fiber-reinforced foamed concrete [29–38]. Previous work examined the behavior of fiber reinforced composites at high temperature, but limited attention has been given to the bond between steel fibers and the cementitious matrix within the range of 400 to 800°C. This range is important because interfacial damage begins to intensify once temperatures exceed 400°C and then progresses rapidly near 400 to 500°C.

The present study addresses this gap through a combined experimental program that includes mechanical pullout testing and microstructural examination using SEM, EDS, and TGA. This approach makes it possible to link the reduction in pullout resistance to specific physical and chemical changes at the interface, such as oxidation, loss of fiber cross section, matrix dehydration, and local separation between the two phases. The findings provide clearer insight into the mechanisms that control the residual performance of steel fiber reinforced mortars after heating and support the development of mixtures with improved fire resistance.

2. Mechanical behavior of fiber mortar at high temperatures

Ezziane et al. [39] examined the thermal properties of different fiber-reinforced mortars, specifically those incorporating steel, polypropylene, and hybrid fibers. The study utilized standardized flexural tests under both oven and flame-induced heating, assessing the changes in flexural strength at elevated temperatures. This study investigates the comparative flexural performance of standard mortar and mortar reinforced with 0.58 % steel fibers when subjected to thermal exposure. The main focus is on flexural strength and residual elastic modulus as important indicators of how well the materials perform under heat and stress.

Figure 1 illustrates the changes in flexural strength of standard mortar and steel fiber-reinforced mortar (SFRM) at different temperatures: 20, 400, 500, and 800°C. At room temperature (20°C), the incorporation of steel fibers markedly improves the flexural strength of the mortar, elevating it from slightly above 8 MPa for standard mortar to nearly 16 MPa for steel fiber reinforced mortar (SFRM). The significant increase in strength is due to the fiber bridging mechanism, which inhibits the propagation of microcracks, thereby enhancing the material's resistance to bending and its energy absorption capacity post-cracking [40–43]. The flexural strength of both materials declines with increasing temperature, with a more significant reduction observed in the steel fiber-reinforced mortar at elevated temperatures. At 400°C, both materials exhibit a decrease in strength, and by 800°C, the SFRM undergoes a notable reduction in strength attributed to fiber oxidation and cement matrix degradation. This underscores the improved fire resistance of steel fibers up to a specific temperature limit, beyond which their performance declines significantly due to damage caused by high temperatures.

There is a lot of proof in the literature that these claims are true. Yoo et al. [44] found that adding up to 3 % steel fibers by volume to ultra-high-performance fiber-reinforced concrete (UHPFRC) makes a big difference in how strong it is when bent and how well it works mechanically overall. Duy-Liem et al. [45] also found that high-performance fiber-reinforced concrete (HPFRC) with steel fibers in it was up to 3.54 times stronger than regular concrete. This shows how

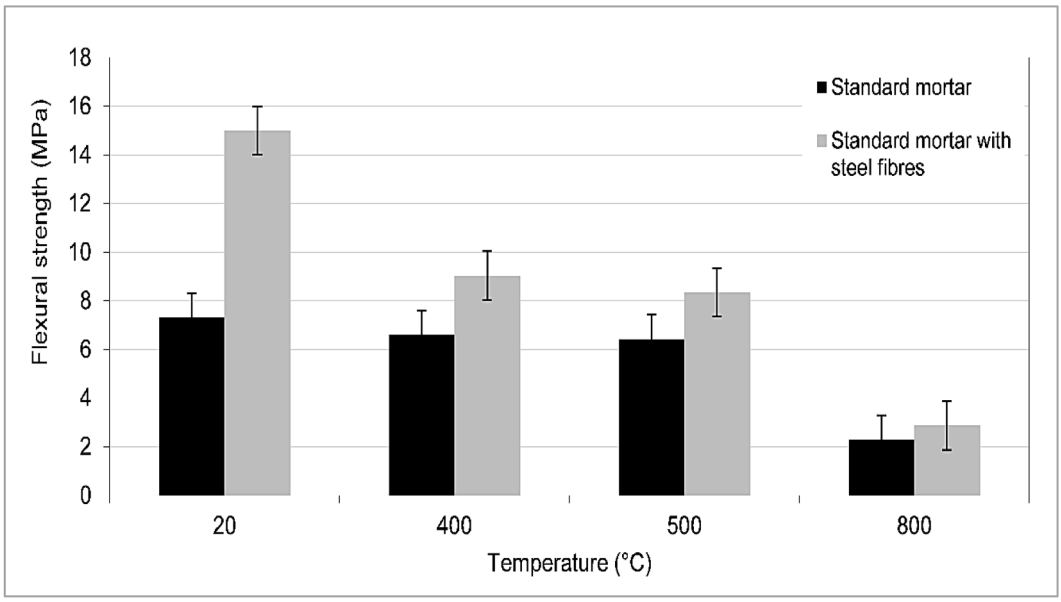

Fig. 1. Variation of flexural strength with respect to temperature.

important fibers are for making things stronger.

To figure out how much better the performance is, it's very important to know what kind and how many fibers were used. For example, Duy-Liem et al. [45] found that hybrid fiber systems that use both macro and micro steel fibers are better at controlling deflection, toughness, and flexural capacity than systems that use only one type of fiber. Ashour and Wafa [46] also said that adding more fibers to beams of high-strength concrete made them much stronger and less likely to break. This shows that there is a strong connection between the amount of fiber used and better ductile behavior [47,48].

Steel fibers not only make things stronger, but they also make them last longer and tougher. Mardani-Aghabaglou et al. [49] and Luo et al. [50] found that mortar and concrete mixtures with fiber reinforcement are better able to handle impact loading, wear and tear, and damage from the environment. This makes them great for use in tough places or situations where they will wear out quickly.

Adding steel fiber has many benefits, but how well it works depends a lot on the properties of the matrix, the shape of the fibers, and how much it is used. Several studies stress how important it is to use the right volumetric ratios and fiber combinations in custom mix designs to get the best performance. This shows how important it is to make designs better so that they work well in the real world while still being easy to use and not too expensive [51,52].

As the temperature rises, the mechanical properties of both plain and fiber-reinforced mortars get worse over time. For example, flexural strength clearly goes down as the temperature rises. Between 400 and 500°C, there is a critical turning point where fiber-reinforced mortar loses about 30 % of its flexural strength. Even though this decline is happening, the steel fibers still help the structure, mostly by bridging cracks and dissipating energy. This means that the mortar doesn't break down as quickly as it would without reinforcement. But once the temperature reaches 500°C, the strength loss speeds up in both materials. At 800°C, the loss of structural capacity is most noticeable, and the fiber-reinforced composite only keeps a small amount of its strength.

This thermal response is very similar to well-known ways that fiber-reinforced cementitious systems break down. The first stage of strength loss is mostly caused by the drying out of the matrix and the breaking down of hydration products, especially calcium hydroxide ($Ca(OH)_2$). This makes the cement microstructure less stable and lowers its internal cohesion [53,54]. Thermogravimetric and calorimetric studies on ultra-high-performance fiber-reinforced concrete back up the idea that chemical phase changes are closely linked to mechanical damage across a wide range of temperatures.

The interface between the fibers and the matrix is another important area of weakness. As the temperature rises, especially above 400°C, the bond between the steel fibers and the surrounding matrix starts to break down. Pang et al. [55] found that the pull-out resistance of straight steel fibers drops a lot as the temperature rises. However, hooked-end fibers keep their performance up to about 400°C before starting to drop off in the same way. This means that the shape of the fiber anchorage helps slow down thermal degradation in the early stages, but it can't completely stop bond failure when the temperature stays high for a long time.

At temperatures close to 800°C, the steel fibers themselves become increasingly important in the processes that break them down. These high-temperature effects make the fibers less mechanically strong and ductile, which makes it harder for them to help the cosmic system's residual strength and load transfer across cracks [54,56]. Steel fibers are naturally more thermally stable than polymeric fibers, but their tendency to oxidize on the surface and lose tensile strength makes them less useful in very hot or cold conditions.

Some researchers have suggested using hybrid fiber systems or thermally stable inorganic fibers to stop this degradation. For example, Zeng et al. [56] found that adding calcium carbonate whiskers to fiber-reinforced matrices can help keep cracks from forming and keep nucleation control up to 600°C, which lowers the loss of strength. Qinghua et al. [57] also said that hybrid reinforcement configurations that combine steel with other fiber types can provide different levels of resistance to degradation at different temperatures.

Figure 2 illustrates the variation in residual elastic modulus for standard mortar and steel fiber-reinforced mortar (SFRM) as a function of temperature, spanning from 20 to 800°C. At room temperature, both materials demonstrate an initial modulus of approximately 38 GPa. Nonetheless, this value exhibits a nearly linear decline with increasing temperature, falling below 5 GPa at 800°C. The incorporation of steel fibers minimally impacts overall stiffness, especially at temperatures exceeding 400°C. This indicates that although the fibers improve the material's crack resistance, they do not substantially alter the inherent stiffness of the cement matrix. The decline in modulus primarily results from microstructural degradation, characterized by matrix shrinkage, crack formation, and pore enlargement due to thermal exposure. The primary factor contributing to the decrease in elastic modulus is thermal

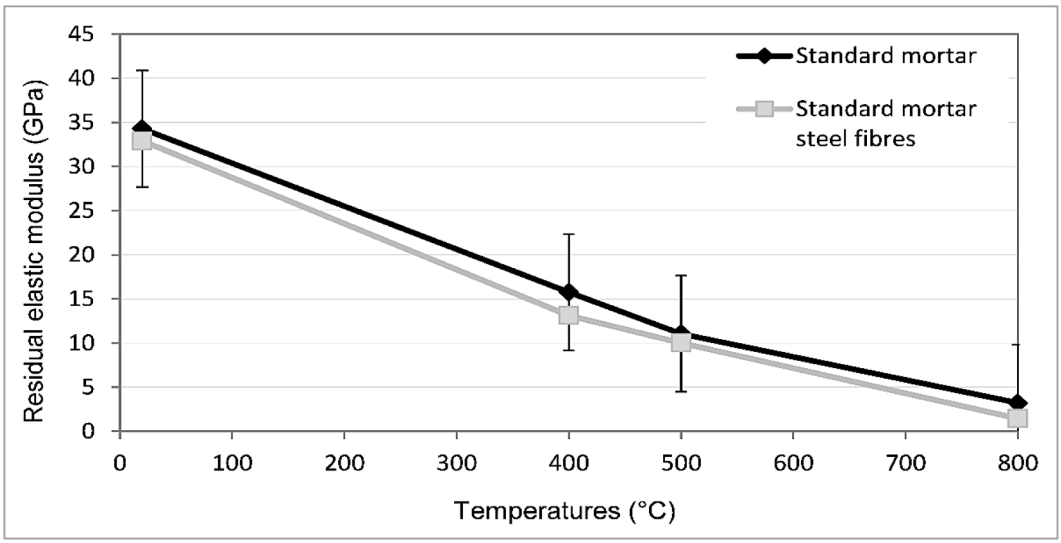

Fig. 2. Variation of elastic modulus with respect to temperature.

damage to the cementitious matrix [58].

It is well known that fibers make cementitious composites stronger and less likely to crack. Fibers make the composite more flexible and better able to handle stress after it has cracked by filling in cracks and redistributing stress. However, their effect on the composite's intrinsic stiffness, which is usually measured by the elastic modulus, is still limited. This is because the cementitious matrix is what makes the whole thing stiff, and it is very easy for the microstructure to break down, especially when it is under thermal or mechanical stress. Matrix shrinkage, crack formation, and pore coarsening all lower the modulus of elasticity, no matter how much fiber reinforcement there is [42,59,60].

The type of fiber and the makeup of the matrix are two important factors that affect how well fiber-reinforced composites work as a whole. For example, Lu et al. [61] said that adding coarse silica sand to PVA and PE fiber-reinforced systems can make the matrix microstructure looser and the pores bigger. This makes it harder for the fibers to spread out and weakens the interface between the fibers and the matrix. In the end, this makes the composite less strong and less uniform. The modulus of elasticity of the fibers themselves also has a big effect on how well they work. If you bend brittle fibers with high stiffness, they may break early. On the other hand, ductile fibers with lower modulus values are more likely to yield locally and keep working well over a wider range of deformation [62].

The microstructural integrity of the matrix is very important for keeping the composite stiff. When a material is pulled apart, one of the main ways it gets damaged is through distributed matrix cracking, which makes it less stiff over time. Mobasher et al. [63] showed that the formulation of the matrix, the curing process, and the age of the fabric-cement composites all have a big effect on how cracks form, including their width, density, and direction. In the same way, shear stress doesn't cause cracks to form in the matrix when there are complicated loading conditions. Instead, axial stress does. This shows that the matrix's natural tensile behavior is a major factor in controlling stiffness [64].

When the matrix is exposed to high temperatures, it breaks down even more. Thermal shrinkage, along with pore coarsening and more microcracking, makes the loss of stiffness worse. Composites made with dense matrices, especially those with additives like silica fume, may be stronger and last longer at first, but they may also be more likely to crack when heated because they don't let heat through as easily and are more brittle [62]. This shows how hard it is to find the right balance between matrix density and thermal resistance.

At approximately 500°C, a critical temperature threshold is noted, indicating a substantial alteration in the behavior of SFRMs. At temperatures below this threshold, the fibers retain mechanical integrity and exhibit strong adhesion to the matrix, thereby preserving their pullout resistance and enhancing the overall structural integrity. As the temperature surpasses 500°C, significant degradation is observed: the oxidation of steel fibers occurs, resulting in a weakened interfacial bond between the fibers and the cement matrix. The oxidation process begins at the fiber surface and intensifies with increasing temperature. The bond strength and flexural strength of the composite material decrease significantly. SEM observations indicate the formation of oxide layers on fiber surfaces and the initiation of interfacial delamination at temperatures exceeding 500°C. The TGA data corroborates these findings, indicating significant mass loss due to oxidation within this temperature range, thereby reinforcing the mechanical results and confirming the considerable degradation of the fiber-matrix bond. The thermal degradation mechanism, influenced by oxidation and the reduction of interfacial adhesion, corresponds with prior research that has established 500°C as a pivotal threshold for the initiation of substantial bond failure in fiber-reinforced composites [65–67]. Adding steel fibers to mortar makes it much more fire-resistant and able to handle cracking at moderate temperatures (≤500°C). However, their effectiveness drops sharply after that point because of chemical and structural degradation mechanisms. This shows how important it is to think about both mechanical benefits and thermal durability when making fiber-reinforced composites for use in fires [68–71].

3. Bonding of steel fibers–cement matrix with respect to temperature

3.1. Experimental methodology

This section addresses the experimental evaluation of the interfacial bond between steel fibers and the cementitious matrix. The integrity of this bond is influenced by both the microstructural quality of the matrix and the physical condition of the embedded fibers, particularly after exposure to elevated temperatures.

To study the evolution of bond performance under thermal stress, prismatic mortar specimens measuring 4 × 4 × 16 cm were prepared. The mortar mix followed a standardized formulation, consistent with the study by Ezziane et al [39], and comprised a water-to-cement ratio (w/c) of 0.5 and a sand-to-cement ratio (s/c) of 3. The hydraulic binder used was CEM I 52.5, and steel fibers were added at a volumetric content

of 0.58 %, ensuring proper workability without the need for superplasticizers. This formulation aligns with the protocol used in previous research, ensuring consistency in the preparation and composition of the mortar specimens for accurate testing and comparison. The geometric and mechanical properties of the fibers are summarized in Table 1.

To ensure the reliability and reproducibility of the results, control measures and sampling mechanisms were carefully followed throughout the study. A minimum of three specimens were tested for each condition to ensure repeatability and minimize variability. The results are presented as averages with corresponding standard deviations to reflect the precision of the measurements. Strict control measures were implemented at every stage, from specimen preparation and curing conditions to thermal exposure, ensuring consistency and reliability in the testing process.

To assess the fiber–matrix bond strength, several experimental protocols are cited in literature, such as direct tension tests using dog-bone specimens [72,73] or pullout tests [74]. However, this study adopts a modified four-point flexural pullout configuration, which is both practical and representative of structural loading conditions.

Custom molds were fabricated to incorporate a cardboard comb that precisely positioned fibers in predefined locations and layers, enabling consistent orientation across specimens. Fig. 3 illustrates the embedding of fibers in one, two, or three horizontal layers within the mortar specimens. The horizontal spacing between fibers in each layer, designated as e, was established at 5 mm to ensure uniform distribution. The initial fiber layer was placed 5 mm above the specimen's base, ensuring uniform anchorage depth among all specimens. This configuration enabled precise fiber positioning, thereby allowing for accurate assessment of interfacial bond strength and mechanical performance across various loading conditions. The organized arrangement of fibers in horizontal layers facilitated effective measurement of bond strength at different depths within the specimen during pullout tests.

Specimens were subjected to controlled thermal treatment at four target temperatures: 20°C (ambient), 400, 500, and 800°C. The heating protocol followed a uniform rate of 5°C/min, with each target temperature maintained for 1 hour to ensure thermal equilibrium. Cooling was conducted passively inside the sealed furnace, following a controlled descent of approximately 0.3°C/min, mimicking realistic post-fire cooling conditions.

Following the treatment process, all specimens were subjected to four-point bending tests, as depicted in Fig. 4, which presents both a detailed schematic diagram and a photograph of the four-point flexural pullout test configuration. Throughout the testing procedure, load and displacement data were continuously recorded using a sophisticated data acquisition system. Two critical parameters were extracted from each test: the load at the first fiber pullout (representing the initial debonding event) and the maximum load immediately prior to the final failure, which corresponds to the complete loss of bond integrity between the fiber and the surrounding matrix.

3.2. Pullout stress with respect to temperature

The average shear stress in the fibers was calculated by making the following assumptions: small deformations in comparison with the overall dimension of the sample, perfect elasticity of the steel fibers at all temperatures, plane sections remain plane, and torsional stiffness of the fibers is negligible.

Under flexural loading, it is postulated that a hinge develops at the upper tensile surface of the specimen, where the mortar matrix becomes entirely cracked and ceases to resist tension. Beyond this cracking point, the entire bending moment is solely resisted by the steel fibers bridging the crack [75–78]. The fibers are embedded within the tensile zone of the beam, organized into distinct horizontal layers as depicted in Fig. 5.

Table 1
Steel fiber properties.

	ϕ (μm)	L (mm)	ρ (kg/m^3)	σ_t (GPa)	E (GPa)	$T_{melting\ point}$ (°C)	α (μ/m)
Fiber	250	25	7850	1 to 3	200	1500	11

The mortar specimen features a rectangular cross-section, with b representing the width and h indicating the overall height of the specimen. In this section, steel fibers are arranged in several parallel layers at depths e_1, e_2, and e_3. The vertical positions of fiber layers are relative to the assumed hinge point. The distances from the hinge to each fiber layer are represented as d_1, d_2, and d_3, which serve as the moment arms for the corresponding fiber forces.

Each fiber layer exerts a tensile force Fi, acting at its respective vertical distance di from the hinge. The total internal resisting moment M_f is the aggregate of the individual moments produced by each fiber layer. The moment equilibrium equation is formally expressed as Eq. (1):

$$M_f = F_1.d_1 + F_2.d_2 + F_3.d_3 = \sum_{i=1}^{i=n} F_i.d_i \tag{1}$$

Where $d_i = h - e_i$

Each fiber layer generates a tensile force F_i as a result of its elongation δ_i, which is induced by rotation at the hinge point and the associated crack opening. Under the assumption of linear elastic behavior of the fibers, the correlation between tensile force and displacement adheres to Hooke's law, which can be expressed as Eq. (2):

$$F_i = K\delta_i \tag{2}$$

Where K is the tensile stiffness coefficient of the fiber. The deformation and geometric compatibility Eqs. (3) and (4) can be written as follows:

$$\frac{F_{i+1}}{F_i} = \frac{\delta_{i+1}}{\delta_i}. \Rightarrow F_{i+1} = \frac{\delta_{i+1}}{\delta_i}.F_i \tag{3}$$

$$\frac{d_{i+1}}{d_i} = \frac{\delta_{i+1}}{\delta_i} \tag{4}$$

Substituting Eq. (4) in Eq. (3) one obtains:

$$F_{i+1} = \frac{d_{i+1}}{d_i}.F_i \tag{5}$$

Equilibrium between the external moment and the force acting on the fibers can be expressed by combining Eqs. (5) and (1). The force $\boldsymbol{F_i}$ can be expressed in terms of the external moment (Equations (6)):

$$M_f = \frac{F_i}{d_i}.\sum_{i=1}^{i=n} {d_i}^2. \Rightarrow F_i = \frac{d_i}{\sum_{i=1}^{i=n} {d_i}^2}.M_f \tag{6}$$

The force F_i represents the tensile load acting of a group of m fibers (in this study m=7); consequently, the load acting on each fiber can be expressed as the following Eq. (7):

$$F_i* = \frac{F_i}{m} = \frac{1}{m}\frac{d_i}{\sum_{i=1}^{i=n} {d_i}^2}.M_f \tag{7}$$

The local interfacial shear stress τ_i quantifies the force transfer between a single steel fiber and the adjacent cementitious matrix. The effectiveness of fiber anchorage is governed by this factor, which directly influences both the pullout resistance and the post-cracking behavior of fiber-reinforced composites [79,80]. Fig. 6 illustrates the anchoring of a single fiber embedded in the matrix, demonstrating that the shear stress is distributed along the lateral surface of the fiber over its embedded length L_f. Under the assumption of uniform stress distribution and ideal bonding conditions, the local shear stress can be expressed as the following Eq. (8):

$$\tau_i = \frac{F_i*}{\pi.\phi.L_f} \tag{8}$$

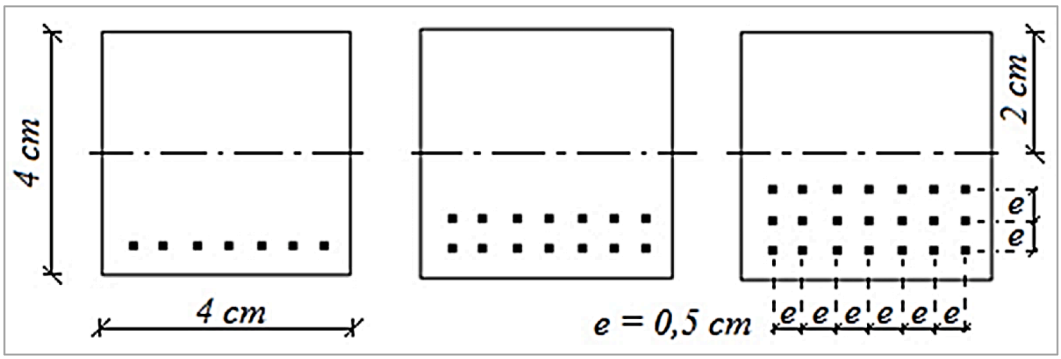

Fig. 3. Position of fibers in one, two or three horizontal layers. The first layer is placed 5 mm from the bottom of the sample and the horizontal spacing of fibers (e) is 5 mm.

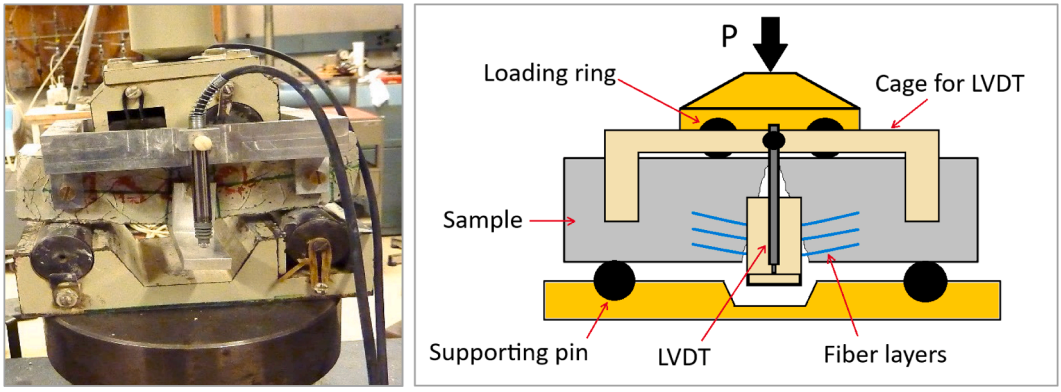

Fig. 4. Fiber pullout test via four-point flexure: (a) Device and (b) Components.

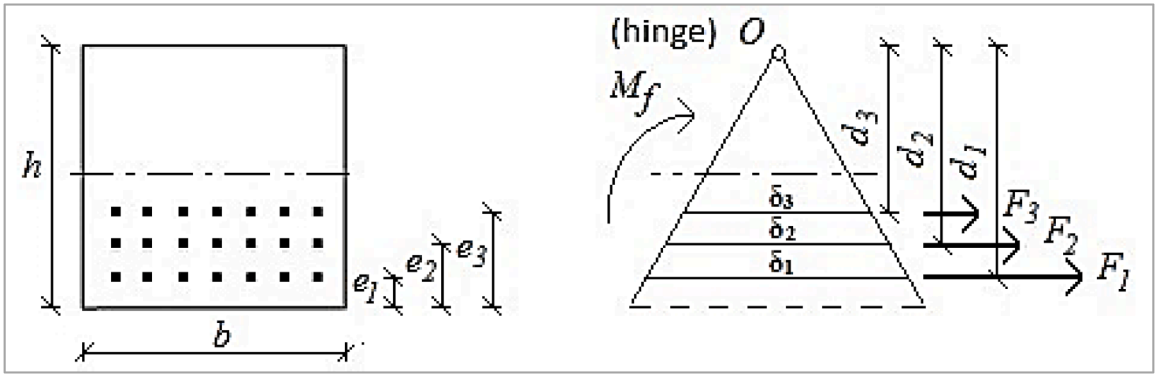

Fig. 5. Cross section and elongation of the fibers.

Where ϕ indicates the fiber diameter. This formulation facilitates a micromechanical evaluation of the bond strength at the fiber–matrix interface and acts as a basis for assessing degradation mechanisms under thermal or mechanical loading. The physical model presented in Fig. 6 supports this interpretation by demonstrating the directionality of shear transfer along the surface of the fiber during tensile loading.

The mechanical response of the fiber–matrix interface under elevated temperatures was assessed by measuring the load at two critical points during four-point flexure testing: (1) the initial pullout of the first fiber, and (2) the maximum load corresponding to the complete debonding of fibers. The calculation of the average interfacial shear stress at these points was performed using the methodology described earlier, specifically employing Eq. (7), which relates the tensile force per fiber to the applied moment, fiber geometry, and distribution.

In these calculations, the effective embedded length of the fibers was taken as 12 mm, and the fiber diameter as 250 μm. For each exposure temperature (20, 400, 500, and 800°C) the reported bond stress values represent the average of nine tests, covering three fiber configurations (one, two, and three horizontal layers), with three specimens tested per configuration.

Fig. 7 illustrates the load-displacement relationship for the tested specimens, providing a comprehensive depiction of the fiber-matrix interaction throughout the pullout process. The curve illustrates the force applied to the steel fibers during their gradual extraction from the cementitious matrix, with distinct indicators for the initial pullout and peak force exertion.

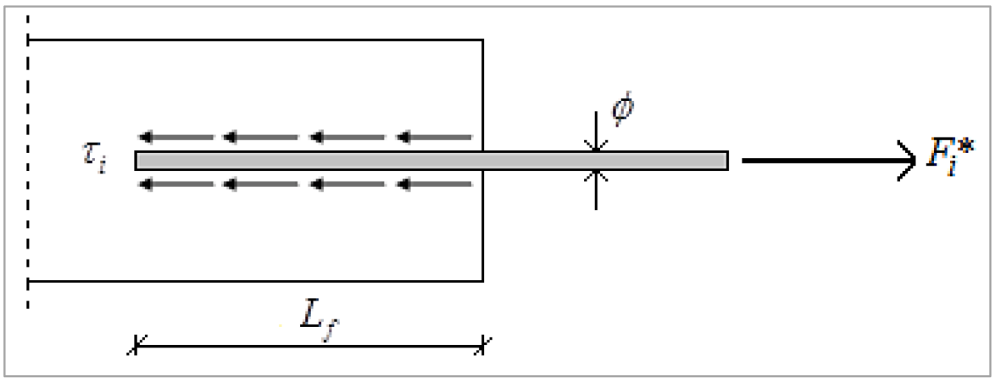

Fig. 6. Anchoring of the fiber in the cement matrix.

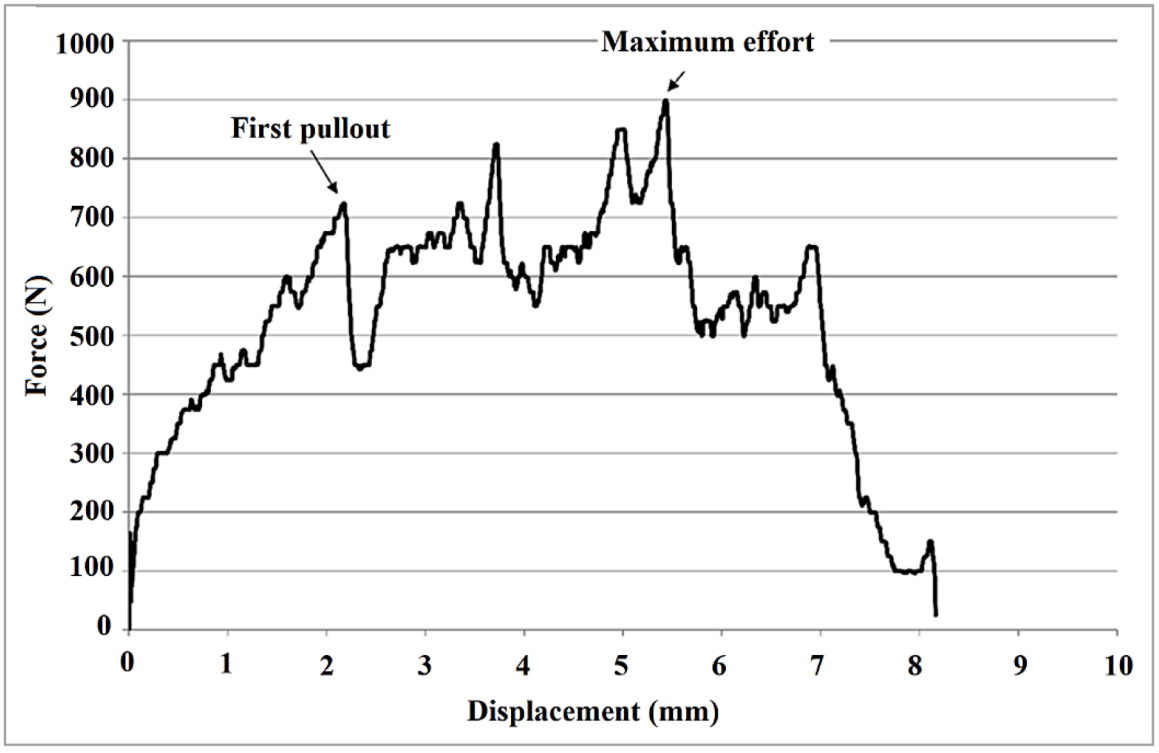

Fig. 7. Variation of force with respect to displacement.

The initial pullout is marked by a decrease in force after reaching the peak value, indicating the moment the fiber starts to separate from the surrounding matrix. This event marks the beginning of bond deterioration, as the interfacial adhesion between the steel fiber and the cement matrix begins to weaken. The force needed to initiate pullout is modest at this stage, indicating a shift from a relatively intact bond to one that is more prone to failure. The initial pullout signifies not a total failure, but the beginning of fiber separation from the matrix, leading to a significant reduction in bond integrity.

The curve subsequently rises until it attains the maximum effort. This point indicates the peak force, defined as the maximum resistance provided by the fiber-matrix bond prior to any additional displacement causing fiber slippage. The force represents the maximum pullout resistance at the interface, where mechanical interlocking and chemical adhesion between the fiber and matrix are fully activated. The maximum effort is essential for comprehending bond strength, as it signifies the point at which the fiber-matrix interaction is most robust. Beyond this threshold, further displacement causes a gradual weakening of the bond, resulting in a significant decrease in force.

Fig. 8 presents the shear stress values associated with the initiation of fiber pullout and the peak load in relation to temperature. The graph illustrates the evolution of interfacial bond strength with temperature, indicating critical points at which bond degradation initiates and advances. The data illustrates the relationship between temperature and bond integrity, which is essential for comprehending the performance and failure mechanisms of steel fiber-reinforced composites in thermal environments.

Results indicate that bond strength remains largely unchanged or exhibits slight improvement between 20 and 400°C when compared to ambient conditions. The observed increase in pullout resistance is due to the shrinkage of the cement matrix, resulting in a more compact microstructure. The transformation of calcium hydroxide [$Ca(OH)_2$] to calcium oxide (CaO) upon moderate heating is pivotal in this process. The chemical transformation that occurs with increasing temperature improves the mechanical interlock between the steel fibers and the cement matrix. The formation of CaO results in matrix densification, which decreases pore space and enhances the bond between the fiber and the surrounding material. Thermogravimetric Analysis (TGA) and

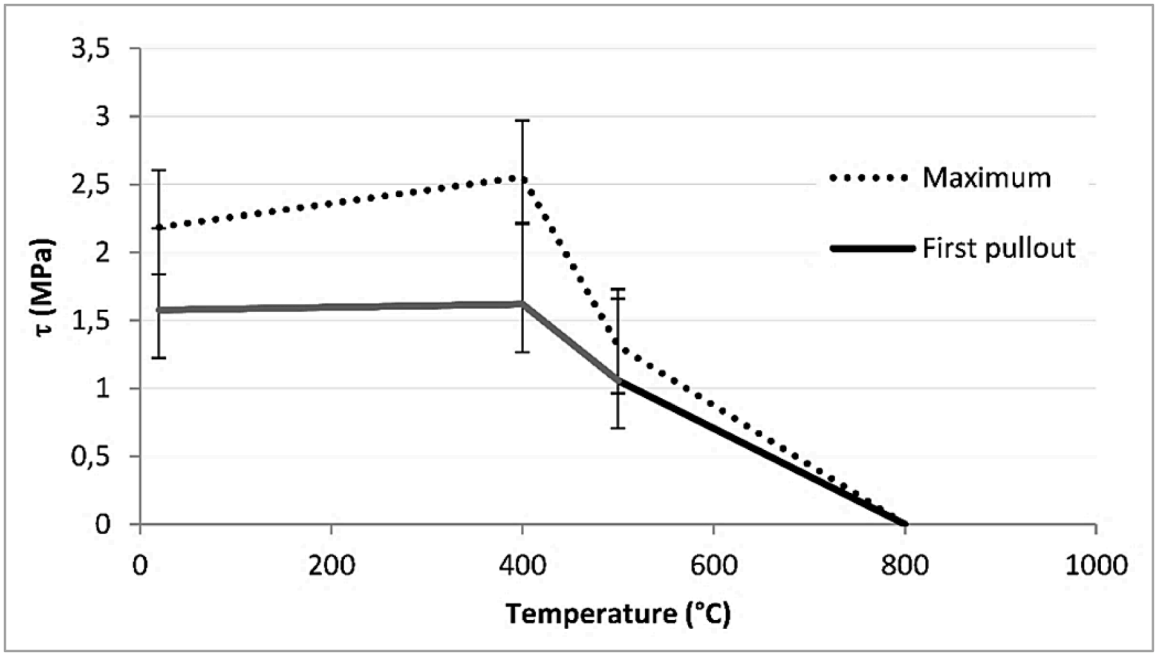

Fig. 8. Variation of shear stress at first fiber pullout and at maximum load with respect to temperature.

Scanning Electron Microscopy (SEM) confirm that this process yields a more stable and stronger interfacial bond at elevated temperatures. The findings align with earlier research [81], which similarly indicates enhanced fiber-matrix anchorage resulting from matrix shrinkage and the thermal transformation of calcium hydroxide at moderate temperatures.

The thermal decomposition of calcium hydroxide ($Ca(OH)_2$) into calcium oxide (CaO) during moderate heating exerts a significant influence on both the microstructural evolution and mechanical performance of cementitious composites. This phase transition alters pore structure and matrix densification, directly affecting shrinkage behavior and internal stress distribution. Consequently, these transformations modulate the mechanical anchorage of embedded fibers within the cement matrix. Depending on the prevailing thermal and chemical conditions, such microstructural reorganization can either enhance interfacial bonding—through improved mechanical interlock and densification—or weaken it due to localized cracking and differential volumetric changes [82].

The shrinkage control potential of CaO has been well documented, especially in alkali-activated slag and fly ash-based systems. L. Zhang et al. [83] demonstrated that incorporating 3 % to 5 % CaO significantly reduced both autogenous and drying shrinkage, with reductions in the latter reaching up to 82 %. This effect is attributed to the formation of crystalline phases, which not only lower the free water content but also coarsen the pore structure, thereby reducing internal tensile stresses during drying. In fiber-reinforced composites, this shrinkage mitigation translates directly to a reduction in microcracking, enhancing the overall dimensional stability and providing a more favorable environment for mechanical fiber anchorage [84].

Beyond shrinkage control, CaO also contributes to improving the fiber–matrix interface. Specifically, the formation of calcium hydroxyzincate (CHZ) crystals at the steel fiber–cement interface, particularly in systems involving zinc-phosphated fibers, has been shown to increase interfacial adhesion. This results in improved flexural performance and enhanced mechanical anchorage by forming a more chemically reactive and mechanically interlocked transition zone [84]. Such mechanisms are critical when evaluating the pullout resistance of fibers in mortars exposed to elevated temperatures.

In addition, recent work has investigated the interaction between low-temperature shrinkable fibers and hydration heat within cementitious systems. W. Wang et al. [85] reported that these fibers, when subjected to early-age thermal activation, induce controlled contraction stress transfer to the matrix, which reinforces the internal structure and improves crack resistance. This highlights a novel synergy between fiber properties and matrix reactivity that may be further optimized in high-performance composites.

While the conversion of $Ca(OH)_2$ to CaO offers valuable benefits in reducing shrinkage and enhancing fiber anchorage, it is not the sole strategy available. Alternative shrinkage mitigation techniques, such as the use of shrinkage-reducing admixtures and sulfoaluminate cement formulations, have demonstrated comparable or superior performance in controlling shrinkage in high-strength fiber-reinforced systems, particularly when tailored to specific water-to-binder ratios [86]. These approaches underscore the importance of a multi-scale material design strategy when aiming to optimize both thermal resistance and mechanical durability in fiber-reinforced cementitious composites.

Above 500°C, however, a steep decline in interfacial shear stress is observed. This is linked to the onset of fiber oxidation, the loss of physical and chemical adhesion, and the progressive dehydration of the cement matrix [16,87]. By 800°C, the fibers are severely corroded, losing a substantial portion of their cross-sectional area. This leads to complete bond failure, with the specimen halves no longer able to transfer load through the embedded fibers. As a result, the calculated pullout resistance effectively drops to zero [22,88,89].

The SEM examination, illustrated in Figs. 9 and 10, substantiates this mechanical degradation by demonstrating considerable oxidation and delamination at the fiber-matrix interface. SEM pictures in Fig. 9 illustrate the development of substantial oxide coatings on the steel fibers, notably noticeable at temperatures over 500°C. The oxide coatings function as a barrier, hindering the adhesion between the steel fibers and the cement matrix. Moreover, Fig. 10 illustrates the emergence of cracks on the fiber surfaces, signifying high-temperature oxidation and the degradation of fiber integrity. The fissures and oxide development at the fiber-matrix interface result in the diminished shear stress, as the fibers can no longer sustain a robust link with the matrix.

The decrease in flexural strength of steel fiber-reinforced mortars at high temperatures, as outlined in Section 2, mirrors the gradual weakening of the link between the steel fibers and the adjacent cementitious

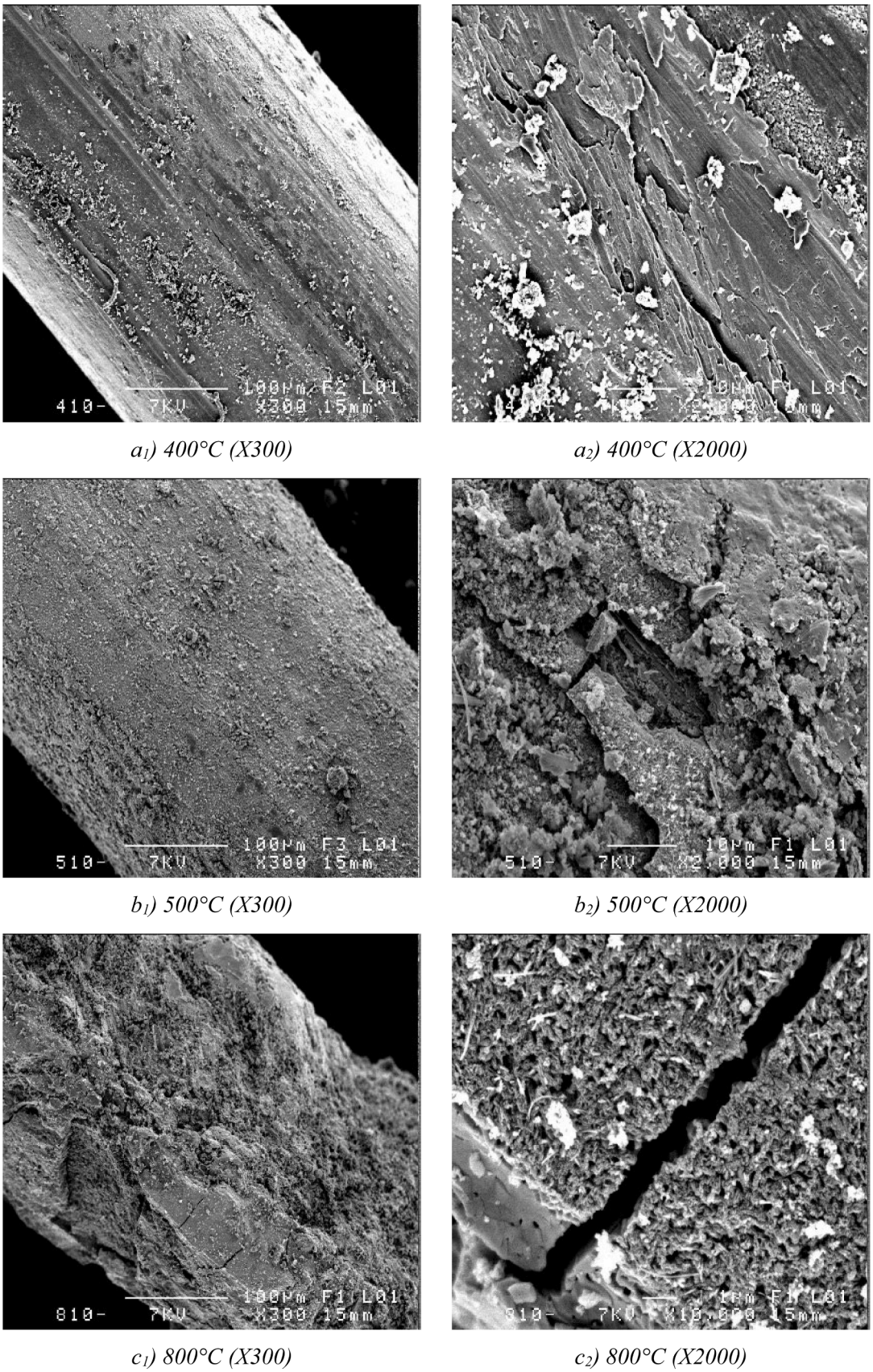

a_1) 400°C (X300) *a_2) 400°C (X2000)*

b_1) 500°C (X300) *b_2) 500°C (X2000)*

c_1) 800°C (X300) *c_2) 800°C (X2000)*

Fig. 9. SEM observation of steel fibers taken from mortar samples subjected to 400, 500, and 800°C.

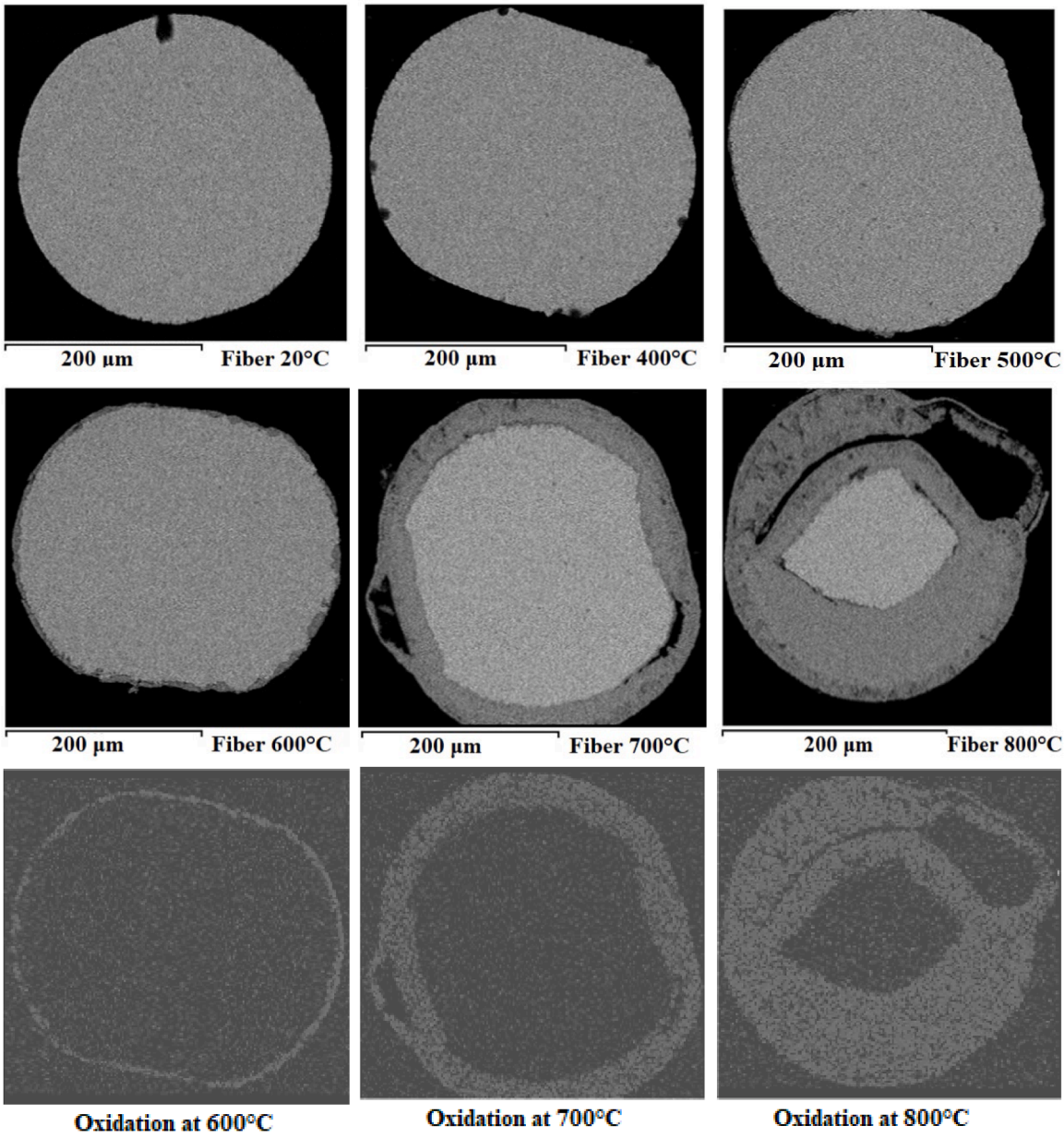

Fig. 10. SEM observation of steel fibers exposed solely to temperature 20, 400, 500, 600, 700, and 800°C; the scale bar corresponds to 200µm. The lower line: oxygen atom mapping which shows the oxidation of the fibers at 600, 700, and 800°C, respectively.

matrix. This correspondence demonstrates a direct mechanical link between macroscopic strength reduction and microscopic interfacial deterioration. As temperature increases, the differential thermal expansion between steel and hydrated cement phases induces internal strains at the fiber-matrix interface, resulting in microcrack initiation and progressive debonding. Concurrently, matrix dehydration and phase transformations—specifically the breakdown of calcium hydroxide and the creation of calcium oxide—diminish cohesive strength inside the interfacial transition zone (ITZ). The combined thermochemical and mechanical impacts impair the fiber's capacity to transfer stress effectively, leading to decreased pullout resistance and a significant reduction in flexural strength. Thus, the deterioration of mechanical integrity at the macroscopic level is primarily due to the gradual breakdown of interfacial bonding, establishing that interfacial degradation is the principal failure mechanism in steel fiber-reinforced mortars exposed to elevated temperatures [55,90–92].

As the temperature rises, the mechanical anchorage of fibers weakens because the microstructure breaks down at the interface. This makes it much harder for the material to transfer loads and stop cracks from spreading. High temperatures cause thermal shrinkage, matrix cracking, and chemical incompatibility, all of which mess up the interface between the fiber and the matrix. Y. Zhang et al. [87] found that the peak pull-out force for steel fibers dropped significantly at high temperatures, which means that the bonding was severely weakened. Fiber geometry also affects the degradation; hooked-end fibers provide better mechanical anchorage than straight fibers, but both types are prone to degradation [16]. These changes directly hurt flexural performance, as shown by several studies that found that the flexural strength of fiber-reinforced mortars steadily decreased as the temperature rose [93].

In Section 2, it was clear that this trend was happening: the strength dropped by 30 % around 500°C, and then it dropped even more after that. These kinds of drops happen because the fibers can't keep bridging cracks when the interface is weak. At first, the presence of fibers makes the composite more ductile and resistant to cracking, but as the interface breaks down from heat, these benefits go away, especially at

temperatures close to 800°C [94]. Comparative results also show that steel fibers break down bonds more than other types of fibers, like carbon or polypropylene, which keep their thermal performance better [93,94]. However, strategies like using hybrid fiber systems, optimizing fiber dosage, and advanced coatings may help to some extent by improving anchorage or delaying interface failure [16].

4. Observations using scanning electron microscopy

Fibers extracted from mortar specimens subjected to combined thermal and mechanical loading were observed using a field emission scanning electron microscope (FE-SEM; Jeol JSM 6301F). The FE-SEM's high spatial resolution facilitated a thorough analysis of fiber surface morphology, revealing microstructural alterations including cracking, surface roughening, and fiber-matrix debonding caused by the combined effects of increased temperatures and mechanical stress. The analyses were crucial for evaluating the integrity and interfacial behavior of the reinforcing fibers within the composite system under complex loading conditions.

Observations were conducted on fiber subjected solely to thermal treatment, without simultaneous mechanical loading. The fibers were analyzed using a conventional scanning electron microscope integrated with an energy-dispersive X-ray spectroscopy (EDS) system (Oxford Link INCA). The conventional SEM enabled morphological assessment, while the integrated EDS provided elemental analysis of surface regions, facilitating the detection of thermally induced chemical changes such as oxidation or phase transformation. This dual-modality characterization method offered a thorough understanding of fiber degradation mechanisms under both isolated and combined stress conditions.

4.1. SEM observations of fibers extracted from the mortar

Fig. 9 shows the SEM observations of steel fibers taken from the mortar samples exposed to the heating - cooling cycle – ambient temperature to 400, 500, and 800°C.

The fibers were taken from the cement matrix after cooling and sample failure. In the case of exposure to 400°C (Fig. 9 (a)) fibers kept their original regular form and showed no formation of cracking on the fiber surface. At a high magnification (image a_2) the microstructure of the material appears little altered and the bonding to the cement matrix appears to be sound. At a temperature of 500°C (Fig. 9 (b)), there is a slight undulation of the fibers without any reduction in section. At high magnification (image b_2) small areas of delamination between the fiber and the cement paste can be seen but without any overall disturbance to the matrix-fiber bond. At this temperature the cement matrix is observed to have its normal morphology. However, at 800°C (Fig. 9 (c)), delamination of the cement matrix and cracking of the fiber are clearly visible (image c_2). At this temperature the fiber is totally altered by the phenomena of oxidation, which has resulted in a loss of physico-mechanic properties cement particles are still visible but some of these particles have started to vitrify.

When the exposure temperature goes up, the microstructure of fiber-reinforced cementitious composites shows that both the fiber-matrix interface and the integrity of the steel fibers slowly but surely get worse. Steel fibers keep their original shape and stay bonded to the surrounding cement matrix at a temperature of 400°C, which is not too high. This suggests that thermal exposure has little effect on microstructural stability at this stage, which is in line with what was found by Mehrdad et al. and Qinghua et al. [54,57]. At 500°C, though, changes in shape, like fiber undulation, become clear, and early signs of interfacial delamination start to show up. Even with these changes, the composite still works well, and the cement matrix still mostly keeps its shape [57,95].

At 800°C, the degradation becomes markedly more severe. Steel fibers exhibit extensive surface cracking, accompanied by pronounced separation from the surrounding cement matrix. These microstructural alterations indicate a fundamental breakdown of interfacial bonding, primarily driven by advanced oxidation of the steel and thermally induced transformations within the matrix. The onset of vitrification where cement particles partially fuse and acquire a glassy morphology further compromises the mechanical interlock between the two phases, significantly diminishing the composite's load transfer capacity and structural integrity [54,96,97].

Chemical and physical processes are mostly to blame for the breakdown of both fibers and the matrix when they are heated. Oxidation makes steel fibers less strong and flexible, and changes in the microstructure, like the cement paste turning into glass at high temperatures, changing the matrix's ability to hold up mechanical loads. These processes work together to make the composite much weaker and less durable at high temperatures [57,96].

Even with these problems, adding steel fiber still makes things work better when they are exposed to moderate heat. For example, steel fibers improve tensile and compressive strength up to a point close to 650°C. After that point, their performance may suffer because of too many fibers and bond deterioration [54]. Also, the interface between the fibers and the surrounding matrix is not the same everywhere. A thin duplex film forms around the reinforcement, which is more sensitive to high temperatures than the bulk paste [96].

4.2. SEM observations of fibers exposed to temperature

Steel fibers were subjected to heat treatment at a range of temperatures (20, 400, 500, 600, 700, and 800°C) following the same standardized protocol used for the mortar specimens. After thermal exposure, the fibers were embedded in resin, sectioned, and polished to obtain a cross-sectional view for detailed examination. The resulting images are shown in Fig. 10, which includes both high-resolution SEM micrographs and oxygen atom mapping of the fiber surfaces at each of the specified temperatures.

To complement the morphological analysis, oxygen atom mapping was employed to visualize the oxidation phenomena occurring on the surface of the fibers. For fibers that were not exposed to elevated temperatures (20°C), the SEM analysis revealed the presence of zinc and phosphorous, indicating the application of a protective anticorrosion treatment, commonly referred to as phosphating or Parkerizing [73]. The SEM images reveal that at 500°C, the oxidation process initiates in a superficial layer around the fibers, characterized by a darker region that is notably less dense in heavy elements. Micro-probe analysis of this darker zone confirmed the presence of ferrous oxide (FeO), a compound that forms at high temperatures, thus corroborating the onset of oxidation at this threshold [98]. Furthermore, the internal region of the fiber, appearing lighter in the SEM images (and consequently richer in iron), remained unoxidized, confirming that the oxidation was confined to the outer surface, and had not yet penetrated deeper into the material.

It is important to note that zinc has a melting point of 420°C, and therefore the protective zinc coating on the fibers is significantly affected above this temperature, leading to the progressive degradation of the protective layer. With rising temperatures, the oxidation of steel fibers becomes more pronounced. At 700°C, the oxide layer on the fibers attains a thickness of approximately 30 μm, increasing to about 75 μm at 800°C. This accounts for approximately 84 % of the original cross-sectional area of fiber. At these extreme temperatures, the oxide layer not only grows thicker but also begins to exhibit significant cracking and detachment from the core of the fiber. These structural changes are visually confirmed by SEM images, particularly Fig. 9 (c2), which clearly shows the extent of the oxide layer degradation and the separation from the steel core. The detachment of the oxide layer from the fiber surface leads to a substantial loss of mechanical integrity. This severe degradation at 800°C results in the complete compromise of the bond between the fibers and the matrix, significantly weakening the fiber's load-bearing capacity.

The upper row of Fig. 10 presents SEM micrographs of the steel fibers

subjected to temperatures of 20, 400, 500, 600, 700, and 800°C, providing a visual progression of the fibers' structural changes with increasing temperature. The lower row, featuring oxygen (O) Ka1 mapping, highlights the oxidation process by visualizing the areas of the fibers that have undergone oxidation at the 600, 700, and 800°C temperature stages. This mapping effectively demonstrates the extent of oxidation as the temperature increases, providing a clear visualization of the fiber's surface degradation under high-heat exposure.

Thermogravimetric analysis of the steel fiber (Fig. 11) was carried out in a synthetic atmosphere (N_2O_2) and showed loss of mass from 450°C which corresponds to the beginning of the previously observed oxidation. At 950°C the loss reached 65 %. In an inert atmosphere (N_2) the loss of mass was virtually zero (less than 0.5 % at 950°C).

When steel fibers are exposed to high temperatures, microstructural and chemical analysis shows that they go through a process of oxidation that weakens their structure over time. The first step in this process is the breakdown of protective surface treatments like phosphating. The last step is the formation of oxide scales, which make fibers brittle and cause mechanical failure. When the temperature and pressure are normal, finding zinc and phosphorus proves that there is a phosphate coating. But this protective layer breaks down above zinc's melting point (420°C), and superficial oxidation starts around 500°C. As the temperature rises, a layer of ferrous oxide (FeO) forms and thickens, which has a big effect on how well the fibers are held in place. Thermogravimetric analysis (TGA) backs this up by showing that mass loss is significant in oxidizing environments, starting at 450°C and reaching up to 65 % at 950°C.

The rates of oxidation and the formation of oxide layers follow a near-parabolic law that is strongly affected by temperature and how long the material is exposed. For example, T91 steel has two layers of oxide scales. The inner layer has more iron and chromium, while the outer layer is mostly made up of iron oxides [99]. At 650°C, different steel alloys show similar behavior, with chromium content having a big effect on oxidation resistance and layer stability [100]. This process speeds up when the protective phosphating treatment breaks down, and oxide layer thicknesses can reach up to 75 μm at 800°C. Also, phosphorus separation at grain boundaries, which has been seen in 12 % CrMoV steels, has been linked to changes in how metals oxidize when they are exposed to high temperatures for a long time [101].

These changes in the microstructure have direct effects on the way things work. As the oxide layer gets thicker, it becomes more brittle and more likely to crack and separate from the metal core. This weakens the fibers and makes them less able to hold onto the metal. The loss of material mass seen in TGA supports the idea that thermal degradation is more severe in oxidizing conditions [100,102]. Alloying elements like chromium make metals less likely to oxidize by forming stable protective layers, but these layers lose their effectiveness when exposed to extreme temperatures for a long time. This shows how important it is to improve alloy formulations and protective surface treatments so that fiber-reinforced cementitious composites can better handle high temperatures and last longer [103,104].

The results show a direct link between temperature rise and the loss of bond between steel fibers and the cementitious matrix. Mechanical tests, SEM observations, and TGA data confirm that the reduction in performance is governed mainly by interfacial degradation rather than changes in the bulk matrix. up to 400°C, the fibers remain anchored and retain their shape, which supports stable flexural behavior and effective crack bridging.

Near 500°C, the first signs of damage appear. Early delamination, changes in fiber shape, and reductions in flexural strength indicate the start of bond failure. SEM images reveal small gaps forming around the fibers, and TGA results show mass loss due to oxidation. These observations match earlier reports that document noticeable drops in pullout strength as temperature increases.

At 800°C, degradation becomes severe. The fibers exhibit heavy oxidation, cracking, and almost complete separation from the surrounding matrix. Vitrification of cement components removes mechanical interlock and prevents stress transfer, which explains the sharp drop in strength. The large oxide layer formed on the fibers corresponds with the significant mass loss recorded in this study.

The overall trend aligns with previous research showing that steel fibers improve performance at moderate temperatures but lose effectiveness once oxidation and thermal mismatch control the response. The findings confirm that interfacial deterioration is the main factor

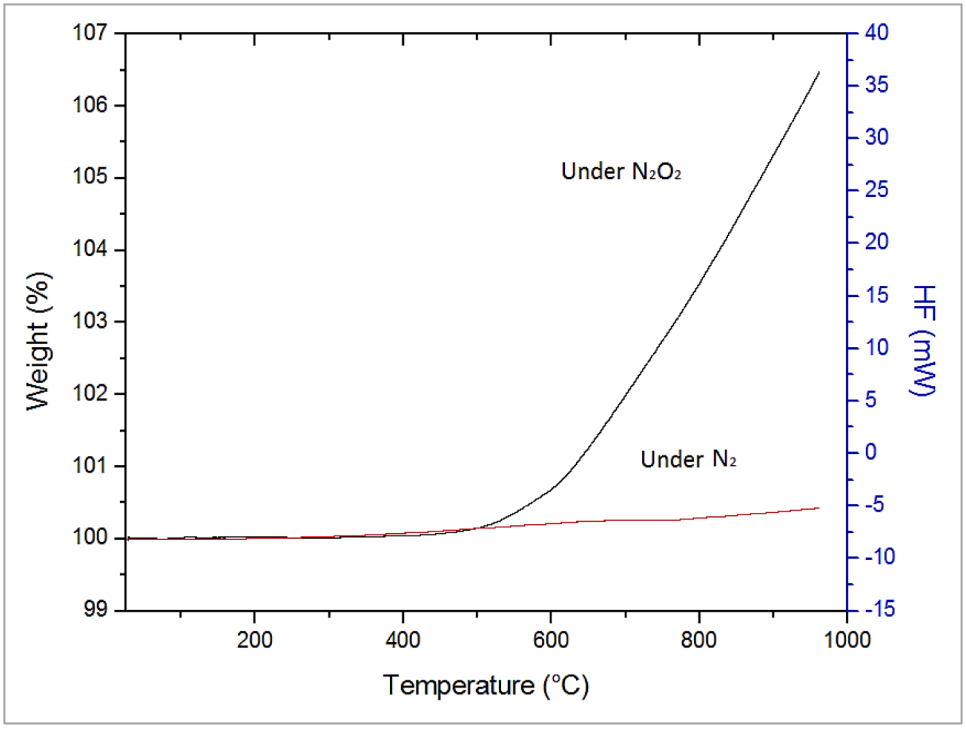

Fig. 11. Thermo-gravimetric analysis of steel fiber.

influencing residual behavior in the range of 500 to 800°C. This insight can guide the development of more stable fiber treatments and reinforcement strategies for improved fire resistance.

5. Conclusion

This work examines the interrelated thermo-mechanical-microstructural behavior of steel fiber-reinforced mortar at elevated temperatures, from ambient temperature to 800°C, employing a multi-scale experimental methodology. The principal conclusions are as follows:

- Mechanical performance remained constant up to 500°C, with steel fibers efficiently bridging cracks and preserving interfacial integrity; however, minor losses in flexural strength and pullout resistance were noted, suggesting initial thermal stability.
- A significant deterioration threshold was seen at around 500°C, where the oxidation and dehydration of the fibers and cement matrix compromised the interfacial transition zone (ITZ), resulting in a marked reduction in mechanical performance.
- At 800°C, significant fiber oxidation led to as much as 84 % of the fiber's cross-sectional area converting into fragile oxide layers, which, coupled with substantial thermal degradation of the cement matrix, resulted in total mechanical support loss and bond failure.
- The results from SEM, EDS, and TGA indicated that the principal factor contributing to performance degradation was interfacial bond failure caused by oxidation, dehydration, and phase transitions in both the steel fibers and the cement matrix, resulting in a 65 % mass loss under oxidizing conditions.
- Although steel fibers enhance heat resistance at mild temperatures, their efficacy declines beyond 500°C. The research highlights the necessity for sophisticated materials, including high-temperature resistant coatings, corrosion inhibitors, and hybrid fiber systems, to improve the endurance of fiber-reinforced cementitious composites in fire-prone settings.

This study provides valuable insights into the behavior of steel fiber-reinforced mortars at high temperatures; nonetheless, it is crucial to acknowledge specific limitations. A key limitation is the utilization of mortar instead of concrete, which does not include the coarse aggregates typically seen in genuine structural concrete. The lack of coarse aggregates in the mortar mixture may affect the mechanical and thermal properties relative to concrete, hence restricting the direct applicability of the results to structural concrete applications. Integrating coarse aggregates into subsequent investigations would yield a more precise depiction of actual conditions. The current study utilizes a specific fiber volume fraction of 0.58 %, which may not represent the complete spectrum of fiber contents commonly employed in practice. The performance of steel fiber-reinforced composites can fluctuate markedly with varying fiber contents, which is essential for optimizing concrete applications. Subsequent research should investigate a wider spectrum of fiber volume fractions and other fiber types to enhance comprehension of how these factors influence the performance of composite materials at elevated temperatures.

To enhance fire resistance, future research should focus on the development of advanced surface coatings and hybrid fiber systems. Silicon carbide (SiC) coatings, known for their exceptional high-temperature resistance, could be applied to steel fibers to significantly reduce oxidation and improve the fibers' durability under extreme heat conditions. Pyrolytic carbon (PyC) coatings present a promising alternative, providing a protective barrier that maintains the thermal stability of steel fibers even in elevated temperatures. In addition, incorporating alternative fibers such as basalt fibers, which offer superior thermal stability compared to conventional steel fibers, or poly(p-phenylene-2,6-benzobisoxazole) (PBO) fibers, known for their outstanding heat resistance and mechanical strength, could further improve the fire performance of fiber-reinforced composites. When combined with improved coatings, these fibers may create hybrid systems that offer enhanced thermal stability and greater durability under fire exposure. Furthermore, exploring fiber surface modification techniques, such as acid treatment, silane coupling agents, plasma treatment, and polymer coatings, could significantly improve the bond strength between fibers and the matrix, leading to enhanced overall performance.

Funding declaration

No funding was received for conducting this study.

CRediT authorship contribution statement

Ezziane M. Mohammed: Writing – original draft, Resources, Methodology, Investigation, Formal analysis, Data curation. **Mohamed Sahraoui:** Writing – review & editing, Validation, Resources, Methodology, Investigation. **Molez L. Laurent:** Writing – review & editing, Validation, Investigation, Formal analysis. **Mostefa Hani:** Writing – review & editing, Validation, Formal analysis. **Ibrahim Messaoudene:** Writing – review & editing, Visualization, Validation. **Yazid Chetbani:** Writing – review & editing, Validation. **Ahmed Belaadi:** Writing – review & editing, Supervision, Investigation. **Ibrahim M.H. Alshaikh:** Writing – review & editing, Validation. **Djamel Ghernaout:** Writing – review & editing, Validation.

Declaration of competing interest

The authors declare that they have no known competing financial interests or personal relationships that could have appeared to influence the work reported in this paper.

Data availability

Data will be made available on request.

References

[1] F. Alsharari, B. Iftikhar, M.A. Uddin, A.F. Deifalla, Data-driven strategy for evaluating the response of eco-friendly concrete at elevated temperatures for fire resistance construction, Results. Eng. 20 (2023) 101595, https://doi.org/10.1016/j.rineng.2023.101595.
[2] S. Peyman, A. Eskandari, Analytical and numerical study of concrete slabs reinforced by steel rebars and perforated steel plates under blast loading, Results. Eng. 19 (2023) 101319, https://doi.org/10.1016/j.rineng.2023.101319.
[3] F. Gong, X. Jiang, Y. Gamil, B. Iftikhar, B.S. Thomas, An overview on spalling behavior, mechanism, residual strength and microstructure of fiber reinforced concrete under high temperatures, Front. Mater. 10 (2023) 1258195, https://doi.org/10.3389/fmats.2023.1258195.
[4] P. Zhang, L. Kang, J. Wang, J. Guo, S. Hu, Y. Ling, Mechanical properties and explosive spalling behavior of steel-fiber-reinforced concrete exposed to high temperature—A review, Appl. Sci. 10 (2020) 2324, https://doi.org/10.3390/app10072324.
[5] P.P. Kalifa P, D. Pardon, F.D Menneteau, C. Gallé, G. Chené, Comportement à haute température des bétons à haute performances: de l'éclatement à la microstructure, Cahier du CSTB, 2002 n°3435.
[6] K. Hertz, Heat-induced explosion of dense concretes, Technical University of Denmark, Department of Civil Engineering, 1984, pp. 1–21.
[7] M. Durmaz, Synergistic effects of steel fibers and silica fume on concrete exposed to high temperatures and gamma radiation, Buildings 15 (2025), https://doi.org/10.3390/buildings15111830.
[8] D. Yang, X. Ren, Y. Gao, T. Fan, M. Li, H. Lv, Study on the basic mechanical properties of waste steel Fiber reinforced concrete after high-temperature exposure, Buildings 15 (2025), https://doi.org/10.3390/buildings15071025.
[9] Q. Zhao, D. Zhang, J. Liu, K. Iwama, P.-F. Zhang, L. Zeng, X.-L. Zhao, Generalized degradation model and bond failure analysis of pultruded basalt/carbon/glass FRP bars and profiles in concrete environments, Adv. Struct. Eng. (2025) 13694332251353604.
[10] Q. Wang, Z. Wang, C. Li, X. Qiao, H. Guan, Z. Zhou, D. Song, Research progress in corrosion behavior and anti-corrosion methods of steel rebar in concrete, Met 14 (2024), https://doi.org/10.3390/met14080862.

[11] L. Zhou, W. Liu, Y. Mao, S. Hou, A diffusion–reaction-deformation cohesive interface for oxidization and self-healing of PyC/SiC interfacial coating, Compos. Struct. 344 (2024) 118332, https://doi.org/10.1016/j.compstruct.2024.118332.
[12] M. Ezziane, S. Bouzouaid, M. Sahraoui, I. Messaoudene, M. Hani, Y. Chetbani, A. Belaadi, I.M.H. Alshaikh, A. Alnmr, D. Ghernaout, Residual performance of Portland cement types-based plain and steel fibre-reinforced mortars exposed to elevated temperatures, Results. Eng. (2025) 107909, https://doi.org/10.1016/j.rineng.2025.107909.
[13] X. Tan, M. Li, L. Zhao, Y. Pan, P. Zhang, M. Qi, Benefits of surface-modified steel fibers on enhancing the mechanical properties in cement matrix, Coatings 15 (2025) 682, https://doi.org/10.3390/coatings15060682.
[14] C. Lin, T. Kanstad, S. Jacobsen, G. Ji, Bonding property between fiber and cementitious matrix: A critical review, Constr. Build. Mater. 378 (2023) 131169, https://doi.org/10.1016/j.conbuildmat.2023.131169.
[15] M. Amran, A.M. Onaizi, N. Makul, H.S. Abdelgader, W.C. Tang, B.T. Alsulami, A. E. Alluqmani, Y. Gamil, Shrinkage mitigation in alkali-activated composites: A comprehensive insight into the potential applications for sustainable construction, Results. Eng. 20 (2023) 101452, https://doi.org/10.1016/j.rineng.2023.101452.
[16] H. Fang, B. Lin, W. Liang, Y. Yao, Constitutive model of interfacial bond-slip between steel fibers and concrete matrix after exposing to high temperature, J. Build. Eng. 77 (2023) 107569, https://doi.org/10.1016/j.jobe.2023.107569.
[17] G.M. Giaccio, R.L. Zerbino, Mechanical behaviour of thermally damaged high-strength steel fibre reinforced concrete, Mater. Struct. 38 (2005) 335–342, https://doi.org/10.1007/BF02479299.
[18] M. Colombo, M. di Prisco, R. Felicetti, Mechanical properties of steel fibre reinforced concrete exposed at high temperatures, Mater. Struct. 43 (2010) 475–491, https://doi.org/10.1617/s11527-009-9504-0.
[19] H. Wang, M. Wei, Y. Wu, J. Huang, H. Chen, B. Cheng, Mechanical behavior of steel fiber-reinforced lightweight concrete exposed to high temperatures, Appl. Sci. 11 (2020) 116, https://doi.org/10.3390/app11010116.
[20] M. Doğruyol, E. Ayhan, A. Karaşin, Effect of waste steel fiber use on concrete behavior at high temperature, Case Studies in Construction, Materials 20 (2024) e03051, https://doi.org/10.1016/j.cscm.2024.e03051.
[21] X. Wu, Z. Cai, Q. Xie, X. Chai, K. Yu, W. Chen, Tensile behavior of high-performance hybrid steel-basalt fibers reinforced cementitious composites after high-temperature exposure, Constr. Build. Mater. 426 (2024) 136059, https://doi.org/10.1016/j.conbuildmat.2024.136059.
[22] D. Zhang, J. Jiang, Y. Weng, D. Wang, X. Wu, S. Fan, Pull-out behaviour of steel fibres embedded in ultra-high-performance concrete after exposure to high temperatures, Constr. Build. Mater. 408 (2023) 133630, https://doi.org/10.1016/j.conbuildmat.2023.133630.
[23] G.T. Caravello, M. Congro, D. Roehl, Experimental and numerical study of damage mechanisms in cementitious materials reinforced with twisted steel fibers, Ibero-Latin American Congress on Computational Methods in Engineering (CILAMCE), 2024.
[24] G. Tong, J. Pang, B. Tang, J. Huang, J. Sun, Mechanisms of mechanical property degradation and dynamic response characteristics of hybrid Fiber reinforced concrete under high-temperature conditions, (2024).
[25] J. Ahmad, Z. Zhou, W. Alattyih, M.T. Naqash, Performance of steel-fibre-reinforced self-compacting concrete subjected to high temperature, Mag. Concr. Res. 77 (2025) 228–240, https://doi.org/10.1680/jmacr.24.00172.
[26] Z. Pi, Z. Wang, H. Xiao, J. Zhou, R. Liu, Tensile performance of cement-based composite reinforced with nano-SiO2 modified steel fiber and its multiscale enhancement mechanism, Constr. Build. Mater. 492 (2025) 143002, https://doi.org/10.1016/j.conbuildmat.2025.143002.
[27] J.J.K. Tchekwagep, Y. Qui, S. Huang, S. Wang, X. Cheng, Studying the mechanical behavior and strengthening of RCSACC after exposure to elevated temperatures, Ing. Investig. 44 (2024) e105573, https://doi.org/10.15446/ing.investig.105573.–e105573.
[28] J. Liu, B. Zhang, W.H. Qi, Y.G. Deng, R.D.K. Misra, Corrosion response of zinc phosphate conversion coating on steel fibers for concrete applications, J. Mater. Res. Technol. 9 (2020) 5912–5921, https://doi.org/10.1016/j.jmrt.2020.03.117.
[29] A. Laouissi, A. Benkhelladi, M. Boumaaza, Y. Karmi, M. Hani, A. Belaadi, R. Zaitri, I.M.H. Alshaikh, D. Ghernaout, Y. Chetbani, Deep neural network modeling of the properties of sustainable high-performance concrete from industrial waste materials, Results. Eng. 27 (2025) 106818, https://doi.org/10.1016/j.rineng.2025.106818.
[30] Y. Kellouche, R. Djebien, A. Laouissi, Y. Karmi, M. Hani, B.A. Tayeh, Y. Chetbani, Prediction and optimization of the compressive strength of marble powder-based concrete using AI techniques: machine learning and metaheuristic approaches, Model Earth Syst Env. 11 (2025) 413, https://doi.org/10.1007/s40808-025-02590-x.
[31] M. Hani, B. Evirgen, Uncoupled thermo-hydro-mechanical modeling of a pykrete diaphragm wall for an alternative artificial ground freezing application, Comput. Geotech. 169 (2024) 106243, https://doi.org/10.1016/j.compgeo.2024.106243.
[32] M. Hani, B. Evirgen, A frozen soil sampling technique for granular soils and thermal modeling, Bull. Eng. Geol. Environ. 82 (2023) 354, https://doi.org/10.1007/s10064-023-03372-4.
[33] M. Hani, B. Evirgen, The mechanical and microstructural properties of artificially frozen Sawdust–Ice mixture (PykRetE) and its usability as a retaining structure, Int. J. Civ. Eng. 21 (2023) 119–134, https://doi.org/10.1007/s40999-022-00751-y.
[34] H. Ben Salah, M. Hani, An investigation of the effect of high temperature on the strength compression and ultrasonic pulse velocity of self-compacting concrete, J. Eng. Exact Sci. 10 (2024) 16818, https://doi.org/10.18540/jcecvl10iss1pp16818.
[35] F. Cheriet, M. Hani, H.A.E. Ladjal, B. Ben aziz, A numerical simulation of slope stability with nailing and shotcreting techniques on natural ground, Model Earth Syst. Env. 10 (2024) 5399–5407, https://doi.org/10.1007/s40808-024-02069-1.
[36] M. Bensmail, R. Zaitri, M. Hani, Y. Chetbani, D. Benamara, A. Laouissi, Analyzing the effects of recycled aggregates on the workability and mechanical characteristics of concrete through mixture design and optimization techniques, World J. Eng. 22 (2025) 1–16, https://doi.org/10.1108/WJE-01-2025-0049.
[37] I. Messaoudene, Y. Chetbani, A. Ouchene, M. Sahraoui, M. Hani, B.A. Tayeh, A. Laouissi, Assessment of the role of blast furnace slag in optimising the physico-mechanical properties of compressed earth blocks stabilised with cement and lime, Eur. J. Environ. Civ. Eng. 29 (2025) 1–24, https://doi.org/10.1080/19648189.2025.2504602.
[38] M. Sahraoui, A. Laouissi, Y. Karmi, A. Hammoudi, M. Hani, Y. Chetbani, A. Belaadi, I.M.H. Alshaikh, D. Ghernaout, AI-driven predicting and optimizing lignocellulosic sisal fiber-reinforced lightweight foamed concrete: A machine learning and metaheuristic approach for sustainable construction, Results. Eng. 26 (2025) 105561, https://doi.org/10.1016/j.rineng.2025.105561.
[39] M. Ezziane, L. Molez, R. Jauberthie, D. Rangeard, Heat exposure tests on various types of fibre mortar, Eur. J. Environ. Civ. Eng. 15 (2011) 715–726.
[40] V. Afroughsabet, L. Biolzi, T. Ozbakkaloglu, High-performance fiber-reinforced concrete: a review, J. Mater. Sci. 51 (2016) 6517–6551, https://doi.org/10.1007/s10853-016-9917-4.
[41] H.Z. Hassan, N.M. Saeed, Fiber reinforced concrete: a state of the art, Discov. Mater. 4 (2024) 101, https://doi.org/10.1007/s43939-024-00171-w.
[42] T.M. Pham, Fibre-reinforced concrete: State-of-the-art-review on bridging mechanism, mechanical properties, durability, and eco-economic analysis, Case Stud. Constr. Mater. (2025) e04574, https://doi.org/10.1016/j.cscm.2025.e04574.
[43] H. Mostafaei, H. Bahmani, D. Mostofinejad, Damping behavior of Fiber-reinforced concrete: A comprehensive review of mechanisms, materials, and dynamic effects, J. Compos. Sci. 9 (2025) 254, https://doi.org/10.3390/jcs9060254.
[44] D.-Y. Yoo, H.-O. Shin, J.-M. Yang, Y.-S. Yoon, Material and bond properties of ultra high performance fiber reinforced concrete with micro steel fibers, Compos. B Eng. 58 (2014) 122–133, https://doi.org/10.1016/j.compositesb.2013.10.081.
[45] N. Duy-Liem, T. Duc-Kien, L.M. Ngoc-Tra, Synergy in flexure of high-performance Fiber-reinforced concrete with hybrid steel fibers, J. Mater. Civ. Eng. 34 (2022) 4022090, https://doi.org/10.1061/(ASCE)MT.1943-5533.0004232.
[46] S.A. Ashour, F.F. Wafa, Flexural behavior of high-strength Fiber reinforced concrete beams, ACI. Struct. J. 90 (1993), https://doi.org/10.14359/4186.
[47] Q. Chunxiang, I. Patnaikuni, Properties of high-strength steel fiber-reinforced concrete beams in bending, Cem. Concr. Compos. 21 (1999) 73–81, https://doi.org/10.1016/S0958-9465(98)00040-7.
[48] M. Kaźmierowski, R. Jaskulski, M. Drzazga, M. Nalepka, M. Kordasz, Effects of the addition of short straight steel fibers on the strength and strains of high-strength concrete during compression, Sci. Rep. 14 (2024) 6989, https://doi.org/10.1038/s41598-024-57574-1.
[49] A. Mardani-Aghabaglou, C. Yüksel, H. Hosseinnezhad, K. Ramyar, Performance of steel micro fiber reinforced mortar mixtures containing plain, binary and ternary cementitious systems, J. Green Build. 11 (2016) 109–130.
[50] X. Luo, W. Sun, S.Y.N. Chan, Steel fiber reinforced high-performance concrete: a study on the mechanical properties and resistance against impact, Mater. Struct. 34 (2001) 144–149, https://doi.org/10.1007/BF02480504.
[51] A.S. Sayyad, R.A. SAYYAD, A review of research on fiber reinforced concrete, J. Mater. Eng. Struct. «JMES» 10 (2023) 581–599.
[52] S. Ali, H. Kumar, S.H. Rizvi, M.S. Raza, J.K. Ansari, Effects of steel fibres on fresh and hardened properties of cement concrete, Civ. Environ. Eng. Rep. 30 (2020), https://doi.org/10.2478/ceer-2020-0039.
[53] T. Way R, K. Wille, Effect of heat-induced chemical degradation on the residual mechanical properties of ultrahigh-performance Fiber-reinforced concrete, J. Mater. Civ. Eng. 28 (2016) 4015164, https://doi.org/10.1061/(ASCE)MT.1943-5533.0001402.
[54] A.M. Mehrdad, I.R. Ali, K. Amir, Microstructural and mechanical characteristics of Fiber-reinforced cementitious composites under high-temperature exposure, J. Mater. Civ. Eng. 34 (2022) 4022208, https://doi.org/10.1061/(ASCE)MT.1943-5533.0004337.
[55] Y. Pang, Q. Tang, Z. Li, D. Gao, L. Yang, D. Liu, D. Li, Bond behaviour between steel fibre and cement mortar exposed to elevated temperature, Mag. Concr. Res. 76 (2024) 1007–1022, https://doi.org/10.1680/jmacr.23.00210.
[56] D. Zeng, M. Cao, X. Ming, Characterization of mechanical behavior and mechanism of hybrid fiber reinforced cementitious composites after exposure to high temperatures, Mater. Struct. 54 (2021) 26, https://doi.org/10.1617/s11527-021-01622-z.
[57] L. Qinghua, G. Xiang, X. Shilang, P. Yu, F. Ye, Microstructure and mechanical properties of high-toughness Fiber-reinforced cementitious composites after exposure to elevated temperatures, J. Mater. Civ. Eng. 28 (2016) 4016132, https://doi.org/10.1061/(ASCE)MT.1943-5533.0001647.
[58] Z.F. Akbulut, T.A. Tawfik, P. Smarzewski, S. Guler, Advancing hybrid Fiber-reinforced concrete: performance, crack resistance mechanism, and future innovations, Buildings 15 (2025) 1247, https://doi.org/10.3390/buildings15081247.
[59] F. Liu, C. Fan, B. Wang, C. Zhou, Z. Chen, Comparative study of interfacial debonding mechanism of fiber pull-out in magnesium phosphate cementitious composites, J. Build. Eng. 102 (2025) 111901, https://doi.org/10.1016/j.jobe.2025.111901.

[60] J. McLean, L. Cui, Multiscale geomechanical behavior of fiber-reinforced cementitious composites under cyclic loading conditions—A review, Front. Mater. 8 (2021) 759126, https://doi.org/10.3389/fmats.2021.759126.
[61] C. Lu, Z. Yuan, C. Yang, D. Hou, Y. Yao, Tensile properties of PVA and PE fiber reinforced engineered cementitious composites containing coarse silica sand, J. Build. Eng. 75 (2023) 106913, https://doi.org/10.1016/j.jobe.2023.106913.
[62] A. Katz, Effect of fiber modulus of elasticity on the long term properties of micro-fiber reinforced cementitious composites, Cem. Concr. Compos. 18 (1996) 389–399, https://doi.org/10.1016/S0958-9465(96)00029-7.
[63] B. Mobasher, A. Peled, J. Pahilajani, Distributed cracking and stiffness degradation in fabric-cement composites, Mater. Struct. 39 (2006) 317–331, https://doi.org/10.1007/s11527-005-9005-8.
[64] V.P. Rajan, F.W. Zok, Matrix cracking of fiber-reinforced ceramic composites in shear, J. Mech. Phys. Solids. 73 (2014) 3–21, https://doi.org/10.1016/j.jmps.2014.08.007.
[65] O.Yavuz Bayraktar, G. Kaplan, J. Shi, A. Benli, B. Bodur, M. Turkoglu, The effect of steel fiber aspect-ratio and content on the fresh, flexural, and mechanical performance of concrete made with recycled fine aggregate, Constr. Build. Mater. 368 (2023) 130497, https://doi.org/10.1016/j.conbuildmat.2023.130497.
[66] H.G. Şahin, Y. Kaya, F.E. Akgümüş, N. Mardani, A. Mardani, J. Assaad, B. Hamad, Degradation of mechanical properties of 3D fiber reinforced printed concrete mixtures exposed to elevated temperatures, Case Stud. Constr. Mater. 22 (2025) e04506, https://doi.org/10.1016/j.cscm.2025.e04506.
[67] S.T. Kang, B.Y. Lee, J.-K. Kim, Y.Y. Kim, The effect of fibre distribution characteristics on the flexural strength of steel fibre-reinforced ultra high strength concrete, Constr. Build. Mater. 25 (2011) 2450–2457, https://doi.org/10.1016/j.conbuildmat.2010.11.057.
[68] H. Jang, H. So, S. So, The properties of reactive powder concrete using PP fiber and pozzolanic materials at elevated temperature, J. Build. Eng. 8 (2016) 225–230, https://doi.org/10.1016/j.jobe.2016.09.010.
[69] M. Abid, X. Hou, W. Zheng, R.R. Hussain, Effect of fibers on high-temperature mechanical behavior and microstructure of reactive powder concrete, Materials 12 (2019) 329, https://doi.org/10.3390/ma12020329.
[70] K.K. Sideris, P. Manita, E. Chaniotakis, Performance of thermally damaged fibre reinforced concretes, Constr. Build. Mater. 23 (2009) 1232–1239, https://doi.org/10.1016/j.conbuildmat.2008.08.009.
[71] S.S. Raza, L.A. Qureshi, Effect of carbon fiber on mechanical properties of reactive powder concrete exposed to elevated temperatures, J. Build. Eng. 42 (2021) 102503, https://doi.org/10.1016/j.jobe.2021.102503.
[72] Y. Lee, S.-T. Kang, J.-K. Kim, Pullout behavior of inclined steel fiber in an ultra-high strength cementitious matrix, Constr. Build. Mater. 24 (2010) 2030–2041, https://doi.org/10.1016/j.conbuildmat.2010.03.009.
[73] M. Sun, D. Wen, H. Wang, Influence of corrosion on the interface between zinc phosphate steel fiber and cement, Mater. Corros. 63 (2012) 67–72, https://doi.org/10.1002/maco.200905580.
[74] S. Hamoush, T. Abu-Lebdeh, T. Cummins, B. Zornig, Pullout characterizations of various steel fibers embedded in very high-strength concrete, Am. J. Eng. Appl. Sci. 3 (2010), https://doi.org/10.3844/ajeassp.2010.418.426.
[75] A. Mudadu, G. Tiberti, F. Germano, G.A. Plizzari, A. Morbi, The effect of fiber orientation on the post-cracking behavior of steel fiber reinforced concrete under bending and uniaxial tensile tests, Cem. Concr. Compos. 93 (2018) 274–288, https://doi.org/10.1016/j.cemconcomp.2018.07.012.
[76] K. Jain, B. Singh, Deformed steel fibres as minimum shear reinforcement–a comparative appraisal, Mag. Concr. Res. 66 (2014) 1170–1182, https://doi.org/10.1680/macr.14.00107.
[77] N.S. Alimrani, G.L. Balazs, Effect of steel fibres on concrete at different temperatures in terms of shear failure, Mag. Concr. Res. 73 (2021) 1113–1124, https://doi.org/10.1680/jmacr.19.00479.
[78] S. Altaan, Z. Thanon, Shear strength of steel fibre self-compacting reinforced concrete beams, in: Proceedings of Eighth International Conference on Concrete in the Low Carbon Era, 2012, pp. 1289–1303.
[79] Z. Yu, W. Liang, M. An, Y. Wang, Ultra-high-performance concrete crack propagation based on fiber random distribution model, Front. Mater. 9 (2022) 857874, https://doi.org/10.3389/fmats.2022.857874.
[80] F. Aslani, S. Nejadi, Bond characteristics of steel fibre reinforced self-compacting concrete, Can. J. Civ. Eng. 39 (2012) 834–848, https://doi.org/10.1139/l2012-069.
[81] B. Georgali, P.E. Tsakiridis, Microstructure of fire-damaged concrete. A case study, Cem. Concr. Compos. 27 (2005) 255–259, https://doi.org/10.1016/j.cemconcomp.2004.02.022.
[82] L. Li, X. Li, B. Wang, J. Tao, K. Shi, A review on interfacial bonding behavior between fiber and concrete, J. Build. Eng. (2025) 112455, https://doi.org/10.1016/j.jobe.2025.112455.
[83] L. Zhang, Y. Ma, X. Ouyang, J. Fu, Z. Li, Effect of CaO on the shrinkage and microstructure of alkali-activated slag/fly ash microsphere, Constr. Build. Mater. 421 (2024) 135672, https://doi.org/10.1016/j.conbuildmat.2024.135672.
[84] V. Corinaldesi, J. Donnini, A. Nardinocchi, The influence of calcium oxide addition on properties of fiber reinforced cement-based composites, J. Build. Eng. 4 (2015) 14–20, https://doi.org/10.1016/j.jobe.2015.07.009.
[85] W. Wang, J. Wu, W. Yang, S. Wang, H. Wu, Z. Zhu, L. Wang, Q. Ding, H. Wang, X. Zhou, Towards low-temperature shrinkable synthetic fibers for internally self-prestressing concrete, J. Build. Eng. 73 (2023) 106769, https://doi.org/10.1016/j.jobe.2023.106769.
[86] A.K.F. Cheung, C.K.Y. Leung, Shrinkage reduction of high strength fiber reinforced cementitious composites (HSFRCC) with various water-to-binder ratios, Cem. Concr. Compos. 33 (2011) 661–667, https://doi.org/10.1016/j.cemconcomp.2011.03.009.
[87] Y. Zhang, J.W. Ju, Q. Chen, Z. Yan, H. Zhu, Z. Jiang, Characterizing and analyzing the residual interfacial behavior of steel fibers embedded into cement-based matrices after exposure to high temperatures, Compos. B Eng. 191 (2020) 107933, https://doi.org/10.1016/j.compositesb.2020.107933.
[88] I. Sæther, Bond deterioration of corroded steel bars in concrete, Struct. Infrastruct. Eng. 7 (2011) 415–429, https://doi.org/10.1080/15732470802674836.
[89] X. Wang, Y. Liu, D.-Y. Yoo, Combined corrosion and inclination effects on pullout behavior of various steel fibers under wet-dry cycle deterioration, Cem. Concr. Compos. 142 (2023) 105229, https://doi.org/10.1016/j.cemconcomp.2023.105229.
[90] R.N. Al-Dala'ien, O. Zaid, M.J. Al-Ezzi, S.R. Wani, State-of-the-art review on high-temperature performance of plant-based fiber reinforced concrete, Discov. Mater. 5 (2025) 176, https://doi.org/10.1007/s43939-025-00379-4.
[91] S.S. Kumar, P. Shyamala, P.R. Pati, D.K. Mishra, V. Sharma, G. Tank, M. Kanan, Investigation and machine learning-based prediction of mechanical properties in hybrid natural fiber composites, Sci. Rep. 15 (2025) 33700, https://doi.org/10.1038/s41598-025-18944-5.
[92] L. Li, P. Jin, K. Zhang, C. Yan, N. Zhang, Y. Li, Q. Feng, Influence of freeze–thaw cycles on fracture behaviors of Nano-SiO2 modified high-strength high-ductility alkali-activated material, Theor. Appl. Fract. Mech. 135 (2025) 104774, https://doi.org/10.1016/j.tafmec.2024.104774.
[93] A. Çavdar, A study on the effects of high temperature on mechanical properties of fiber reinforced cementitious composites, Compos. B Eng. 43 (2012) 2452–2463, https://doi.org/10.1016/j.compositesb.2011.10.005.
[94] Ö. Biricik, S.H. Bayqra, Y. Kaya, A. Mardani, Assessment of mechanical properties of fiber reinforced cementitious system exposed to high temperature, Struct. Concr. 24 (2023) 4733–4750, https://doi.org/10.1002/suco.202200961.
[95] I. Messaoudene, M. Sahraoui, M. Boumaaza, M. Hani, A. Belaadi, S. Mezaouri, Y. Chetbani, I.M.H. Alshaikh, R. Alouani, B. Khalfaoui, D. Ghernaout, Eco-optimized ternary mortars incorporating industrial waste: mechanical performance, statistical, microstructure, and life cycle impact, Case Stud. Constr. Mater. 23 (2025) e05514, https://doi.org/10.1016/j.cscm.2025.e05514.
[96] A. Bentur, S. Diamond, S. Mindess, The microstructure of the steel fibre-cement interface, J. Mater. Sci. 20 (1985) 3610–3620, https://doi.org/10.1007/BF01113768.
[97] L. Li, X. Chaopeng, C. Mingli, Z. Xiongxiong, L. Zongli, Synergistic effect between CaCO3 whisker and steel-PVA Fiber cocktail in cement-based material at elevated temperature, J. Mater. Civ. Eng. 34 (2022) 04021415, https://doi.org/10.1061/(ASCE)MT.1943-5533.0004103.
[98] G. Vourlias, N. Pistofidis, K. Chrissafis, High-temperature oxidation of precipitation hardening steel, Thermochim. Acta 478 (2008) 28–33, https://doi.org/10.1016/j.tca.2008.08.006.
[99] S. Das, S. Sanyal, P. Halder, A. Varma, Y. Ravi Kumar, S. Mandal, Oxide scale characterization and study of oxidation kinetics in T91 steel exposed to dry air at high temperatures (873–1073 K), Met. Mater. Int. 28 (2022) 1864–1880, https://doi.org/10.1007/s12540-021-01088-2.
[100] J. Burja, B. Šetina Batič, B. Žužek, T. Balaško, High-temperature oxidation of boiler steels at 650°C, Met 13 (2023) 1887, https://doi.org/10.3390/met13111887.
[101] M. Mackenbrock, H.J. Grabke, Grain-boundary segregation of phosphorus and micro-structural changes in the steel X 20 CrMoV 12 1 during long-term application at elevated temperatures, Steel Res. 62 (1991) 371–378, https://doi.org/10.1002/srin.199101313.
[102] K. Hannawi, H. Bian, W. Prince-Agbodjan, B. Raghavan, Effect of different types of fibers on the microstructure and the mechanical behavior of Ultra-high performance Fiber-reinforced concretes, Compos. B Eng. 86 (2016) 214–220, https://doi.org/10.1016/j.compositesb.2015.09.059.
[103] K. Beck, A.S. Ulrich, N. Thor, C. Oskay, M.C. Galetz, Chromium diffusion coatings for improving the oxidation behavior of refractory metals at intermediate temperatures, Int. J. Refract Met. Hard Mater 121 (2024) 106626, https://doi.org/10.1016/j.ijrmhm.2024.106626.
[104] D. Schmidt, M.C. Galetz, M. Schütze, Ferritic–martensitic steels: improvement of the oxidation behavior in steam environments via diffusion coatings, Surf. Coat. Technol. 237 (2013) 23–29, https://doi.org/10.1016/j.surfcoat.2013.09.018.